213 nm Ultraviolet Photodissociation on Peptide Anions: Radical-Directed Fragmentation Patterns

Mohammad A Halim, Marion Girod, Luke Macaleese, Jérôme Lemoine, Rodolphe Antoine, Philippe Dugourd

213 nm Ultraviolet Photodissociation on Peptide Anions: Radical-Directed Fragmentation Patterns

Mohammad A. Halim,[1] Marion Girod,[2] Luke MacAleese,[1] Jérôme Lemoine,[2] Rodolphe Antoine,[1] Philippe Dugourd[1]

[1]Institut Lumière Matière, Université Lyon 1 – CNRS, Université de Lyon, 69622 Villeurbanne Cedex, France

[2]Institut des Sciences Analytiques, Université Lyon 1 – CNRS, Université de Lyon, 69622 Villeurbanne Cedex, France

Correspondance to: Philippe Dugourd, Email : phillipe.dugourd@univ-lyon1.fr

Citation : 213 nm Ultraviolet Photodissociation on Peptide Anions: Radical-Directed Fragmentation Patterns. M. A. Halim, M. Girod, L. MacAleese, J. Lemoine, R. Antoine and P. Dugourd. *J. Am. Soc. Mass Spectrom.* **27**, 474-486 (2016). http://dx.doi.org/10.1007/s13361-015-1297-5

Abstract

Characterization of acidic peptides and proteins is greatly hindered due to lack of suitable analytical techniques. Here we present the implementation of 213 nm Ultraviolet photodissociation (UVPD) in high-resolution quadrupole-Orbitrap mass spectrometer in negative polarity for peptide anions. Radical-driven backbone fragmentation provides 22 distinctive fragment ion types, achieving the complete sequence coverage for all reported peptides. Hydrogen-deficient radical anion not only promotes the cleavage of C_α–C bond but also stimulates the breaking of N–C_α and C–N bonds. Radical-directed loss of small molecules and specific side-chain of amino acids are detected in these experiments. Radical containing side-chain of amino acids (Tyr, Ser, Thr, and Asp) may possibly support the N–C_α backbone fragmentation. Proline comprising peptides exhibit the unusual fragment ions similar to reported earlier. Interestingly, basic amino acids such as Arg and Lys also stimulated the formation of abundant b and y ions of the related peptide anions. Loss of hydrogen atom from the charge-reduced radical anion and fragment ions are rationalized by time-dependent density functional theory (TDDFT) calculation, locating the potential energy surface (PES) of $\pi\pi^*$ and repulsive $\pi\sigma^*$ excited states of a model amide system.

Keywords: Photo-fragmentation, Radical Anions, UVPD, Peptide, TDDFT

Introduction

Alternative to collision [1-3] and electron [4, 5] based techniques, photon-based methods have emerged as new powerful approaches for characterizing peptides, polysaccharides and proteins [6-12]. Among them, ultraviolet photodissociation (UVPD) leads to intense fragmentation patterns. In this method, protein and peptide cations predominately dissociate to a/x ions and less frequently to c/z and b/y ions. Different wavelengths such as 157, 193, 220, and 280 nm have been implemented in UVPD. Above and at 280 nm, specific fragmentation have been reported following excitation of aromatic residues in peptides or proteins [13]. The number of fragment ions increases as the wavelength decreases from 280 nm to 213 nm [13, 14].

Another efficient and popular wavelength 193 nm has been implemented in hybrid linear ion trap-orbitrap mass spectrometer for characterizing different peptide and proteins in positive polarity. Wide-ranging fragmentation yields a/x, b/y, c/z, y-1, v, w and d ions and thus provides nearly complete sequence coverage. Whole protein characterization has been achieved by this technique implementing direct infusion and/or chromatographic time scale [15, 16]. Along with common fragment ions, Madsen *et al* also observed some uncommon fragment ions such as a+2, c-1 and z+1 [17]. This study disclosed that fragmentation patterns varied with the protonation state of the peptide. When protonation takes place at N-terminus, cleavage of C_α-C bond occurred, however, N-C_α cleavage is favored with C-terminus protonation.

Thompson *et al* employed vacuum photodissociation at 157 nm on singly protonated peptide ions to elucidate the unusual backbone cleavage [18]. Cui *et al* further revealed that basic residues in the C-terminal yields to x, v and w fragment ions whereas N-terminal produces a and d fragments ions [19]. Moreover, a+1 and x+1 radical ions are identified from the charge localized N- and C-terminals, respectively. Secondary radical elimination of hydrogen atom are detected from a+1 and x+1 ions to produce a and x ions, respectively. Satellite ions such as d, v and w are formed due to part of side chain elimination. b, c and z fragment ions are also noticed but are less frequent than a and x ions. Hydrogen/deuterium exchange experiments further confirmed that both backbone amide and side-chain β-carbon hydrogens can undergo elimination to yield a and x ions [20]. Implementing time-resolved photodissociation at 157 nm revealed some unusual but stable x+2 fragment ion compared to less common a+2 ion [21]. They proposed that addition of one hydrogen

to x+1 and a+1 radical ions can yield x+2 and a+2 ions. Migration and transfer of hydrogen atom to radical ions have also been witnessed in ECD studies [22], [23].

However, most of these experiments were conducted on peptide and protein cations and very few were directed on negative polarity. It is assumed that around 50% of naturally occurring peptides are acidic and prone to yield negative ions. Kjeldsen *et al* reported C_{α}-C backbone fragmentation by EDD (electron detachment dissociation) for peptide and observed more C-terminal species (x ions) than N-terminal fragments ($a^{\bullet}$ ions) [24]. Comparison of negative electron transfer dissociation (NETD) and UVPD for peptide anion disclosed that NETD usually produce simple set of a/x ions [25]. In NETD, along with a/x ions various neutral losses are observed from entire or partial side-chain cleavage of amino acids [26]. Activated ion negative electron transfer dissociation (AI-NETD) of doubly charged peptide ions also generates some hydrogen loss from a and x fragment ions [27].

Some previous electron photo-detachment dissociation (EPD) studies were performed with UV lasers on peptides and small proteins in negative polarity [28, 29]. Antoine *et al* investigated the electron photo-detachment dissociation of peptides using 262 nm with a linear ion trap [30]. Formation of $[M-2H]^{-\bullet}$ radical anion from the precursor ion was documented in this experiment. a/x and c/z fragment ions were observed [28]. Comparative studies between EDD and EPD revealed significantly different fragment ion distributions in which EPD fragment ions are typically produced from tryptophan and histidine resides whereas in EDD backbone dissociation are favored [28]. However, EDD on small proteins including ubiquitin and melittin suggests that basic resides may promote the formation of a/x fragment ions [31].

Radical containing peptides promote characteristic fragmentation pattern in mass spectrometry [32, 33]. Radical peptides are classified into two categories: hydrogen-deficient and hydrogen-rich radicals [34]. The former type is typically formed in UVPD, EDD and NETD routes whereas the later one is generated from ECD/ETD [8, 24, 35-37]. Recently, formation of hydrogen-deficient species from the hydrogen-rich radical cation in ECD received great attention due to extensive fragmentation and wide-spread side-chain loss [33, 38]. Radical migration in hydrogen-deficient peptide radical promotes extensive neutral loss and allows remote backbone dissociation [33, 39].

Here, we present the implementation of 213 nm UVPD in a Thermo Scientific Q Exactive hybrid quadrupole-orbitrap mass spectrometer in negative polarity for peptide anions. We observed distinctive C_α–C, N–C_α and C-N backbone fragmentations from the hydrogen-deficient radical anions. Radical-driven extensive neutral loss is likewise evident in these experiments. Moreover, series of hydrogen-deficient and hydrogen-rich fragments are observed.

Material and Methods

Photodissociation Mass Spectrometry

All experiments were performed on a hybrid quadrupole-orbitrap Q-Exactive® mass spectrometer (Thermo Fisher Scientific, San Jose, CA, USA) equipped with a HESI ion source. Three small peptides YTIAALLSPYS, DYKDDDDK and RGDSPASSKP were used without any further purification. Peptides samples were prepared at 1 µM concentration in 50/49/1 (v/v/v) acetonitrile/water/ammonium hydroxide and directly infused to MS at a flow rate of 5 µL/min. All spectra were acquired using a mass range of 100-1500 *m/z* and resolving power of 140000 at *m/z* 400. The AGC (Automatic Gain Control) target for MS/MS was set to $1x10^6$ and the maximum injection time was set at 250 ms. The isolation width was 2 Th. When required, the identification of fragment ions was confirmed by fragmentation of a single isotope (selection width 0.4 Th). The HCD collision energy was set to the minimum 2 eV in order to avoid collisions and provide photofragmentation spectra free of CID contamination. Different HCD (High Collision Dissociation) trapping times including 100, 500, 1000 and 2000 ms (2, 10, 20, 40 laser shots, respectively) were considered. All experiments were performed on 5 microscans mode with averaging 200 scans.

For UVPD experiments, BrillantB Nd:YAG (Quantel, Les Ulis, France) laser was employed. Details of the set-up are given elsewhere [14]. In brief, the 5^{th} harmonic (λ=213 nm) with a repetition rate of 20 Hz was used. The hybrid quadrupole-orbitrap Q-Exactive® mass spectrometer was modified to permit the laser irradiation of peptide ions. The laser beam passes through lenses, diaphragms and then is introduced in the HCD cell using two dichroic mirrors. A UV grade fused-silica window was fitted on the back of the HCD cell to allow penetration of a laser beam. The laser beam energy irradiating the ions was ~1 mJ/ pulse. The laser was slightly off axis so as to avoid photofragmentation in the C-trap.

Manual analysis of UVPD data was performed with the aid of ChemCalc software [40]. Peak lists of three peptides were generated for all six major UVPD ion types (a, b, c, x, y, and z). Fragments mass tolerance was set to 20 ppm.

Computation

All calculations were conducted with the Gaussian 09 software package [41]. Optimization and subsequent vibrational frequency calculation on the model amide system [$CH_3CONHCH_3$] were performed using density functional theory employing Becker's (B3) [42] exchange functional combining Lee, Yang, and Parr's (LYP) [43] correlation functional. Gaussian basis set 6-311+G (2d,p) was considered. Natural bond orbitals (NBO) [44, 45] calculations were computed at the same level of theory. For calculating the excited state properties, time-dependent density functional theory (TDDFT) [46] was employed with the B3LYP/6-311+G(2d,p) level of theory in gas phase. For TDDFT calculation, 20 excited states were considered.

Result and Discussion

The Photodissociation of Peptide 1 (YTIAALLSPYS)

The photodissociation spectrum of the doubly-deprotonated $[M-2H]^{2-}$ (*m/z* 597.8057) of this peptide is presented in **Figure 1A**. Exact masses and assignments of fragment ions of this peptide are summarized in **Table 1**. Similar to previous studies, the characteristic $[M-2H]^{-\bullet}$ charge-reduced radical species is detected at *m/z* 1195.6094 Da. This radical species is typically generated from photo-induced electron detachment from the selected peptide precursor. Intense neutral losses are detected from this radical species (**Table 2** and **Figure 2)**. Similar neutral losses are also demonstrated in previous studies [30, 31, 47-49]. The CH_3 radical (15.0242 Da) loss appears at *m/z* 1180.5852 from the side-chain of Ala [50]. Neutral loss of CO (27.9947 Da) and CH_3CH_2 (28.9995 Da) are noticed at *m/z* 1167.6147 and 1166.6099 Da, respectively. Removal of CH_3CH_2 can be used to distinguish the side chain loss of Ile (28.9995 Da) or Leu (43.0542 Da) [51]. Loss of CH_2O (30.0100 Da) and CH_2OH (31.0178 Da) are also observed from the side chain of Ser. NETD study on serine (Ser) containing peptide witnessed the loss of CH_2O when Ser is not phosphorylated [26]. The peak at *m/z* 1151.5829 can be assigned to the loss of C_2H_4O (44.0265 Da) from Thr side-chain

[26, 50]. The sequential loss (61.9998 Da) of CO_2 and H_2O is also identified at *m/z* 1133.6099. Radical elimination of a C_3H_8ON from the Thr residue may lead to the fragment ion detected at *m/z* 1121.5759. Loss of tyrosylate groups from the side chain of Tyr (107.0472 and 106.0406 Da) is identified at *m/z* 1088.5622 and 1089.5688 Da, respectively. The phenoxy group of the tyrosylate produces an oxygen radical, which induces the cleavage of C_α-C_β side-chain of the tyrosine residue and promotes the formation of $O=C_6H_4=CH_2$ (exact mass 106.0413 Da) ion [8, 50, 52]. Two relatively weak peaks at *m/z* 1139.5855 and 1123.5910 can be assigned for the side-chain and related ion loss (56.0239 and 72.0184 Da) from Leu or Ile [26, 51-53]. Combined losses of tyrosylate and C_2H_4O from Tyr and Thr appear at *m/z* 1045.5419 and 1044.5346 respectively.

Zooms of **Figure 1A** are shown in **Figure 1B-1C and S1**. Selected fragment ions from the single isotope selection of the doubly-deprotonated $[M-2H]^{2-}$ precursor ions are shown in **Figure S2**. For peptide 1, a series of radical $(a_n+1)^{-\cdot}$ fragment ions is observed for n=5, 6, 7, 8 and 9 These ions correspond to the elemental composition of a_n ions plus one hydrogen atom (explaining the +1 in the notation) and are radicals (dot in the notation).This nomenclature is in agreement with the one proposed recently by Chu et al [54] excepted that we do not include the hydrogen symbol (H) after the number of losses or gains. Homolytic cleavage between the C_α and the carbonyl C from the precursor ion induced the formation of these radical ions, as shown in **Scheme 1**. Classical $(a_n)^-$ fragment ions are detected for n=8 and 9. These ions may mainly arise from the fragmentation of the doubly-deprotonated $[M-2H]^{2-}$ precursor ion. However, they can also be produced by secondary H elimination from the radical $(a_n+1)^{-\cdot}$ fragment ions [19]. Abundant a ions are favored by aromatic amino acids and in this case it is due to Tyr residue in N-terminal [28, 52]. An unusual fragment such as $(a_8+2)^-$ is additionally identified at *m/z* 805.4815 and which may be due to the presence of Pro residue [14, 17]. Detection of $(a+2)^-$ is also reported by Madsen *et al* in a high-throughput UVPD study in negative polarity for complex proteomic sample [55]. Two peaks at *m/z* 871.5031 and 856.4917 correspond to the loss of CH_3CH_2 (28.9995 Da from Ile) and C_2H_4O (44.0265 Da from Thr) from $(a_9)^-$ ion. Radical $(x_n+1)^{-\cdot}$ ions are also formed via homolytic cleavage of the C_α - carbonyl C bond, complementary to $(a_n+1)^{-\cdot}$ ions (**Scheme 1**). Series of radical $(x_n+1)^{-\cdot}$ ions are noticed at n= 2, 5, 6, 7, 8, and 10 whereas $(x_n)^-$ ions are detected at n= 6, 7, 8 and 9. Two unusual fragment types such as $(x_n+2)^-$ for n=2, 8 and radical $(x_n-1)^{-\cdot}$ for n=7 and 9 appear for peptide 1. $(x_2+2)^-$ ion detected at *m/z* 295.0924 is close to Pro residue [14]. Kim and Reilly found x_n+2 fragment ions at 157 nm UVPD and concluded that some x+1 radical ions may take one hydrogen

to form these new ions [21]. $(x_n+2)^-$ ions are also detected at 193 nm UVPD [55]. The proposed fragmentation pathway for the formation of $(x_2+2)^-$ ion is presented in **Scheme 2**.The formation of two $(x_n-1)^{-\cdot}$ ions are likewise owing to the radical elimination of hydrogen atom from the corresponding x_n ions. Shaw *et al* also observed some $(x_n-1)^{-\cdot}$ ions in activated ion negative electron transfer dissociation [27]. Moreover, classical fragmentation of the C_α - C bond with proton transfers from the charge-reduced $[M-2H]^{-\cdot}$ radical species also yields to the formation of $(x_n-1)^{-\cdot}$ ions. Indeed, these ions will contain the initial radical site and the negative charge. Fragmentation is then observed after electron photo-detachment.

Series of $(y_n)^-$ ions are detected at n=2, 3, 6, 7, and 8. Radical $(y_n-1)^{-\cdot}$ ions are also observed at the positions n=6, 7, 8, and 10. These ions arise from the homolytic cleavage of the C-N bond from the precursor ion (**Scheme 3**). However, complementary $(b_n+1)^{-\cdot}$ radical ions are not detected. Fragmentation of the C-N bond from the charge-reduced $[M-2H]^{-\cdot}$ radical species may also leads to the formation of the $(y_n-1)^{-\cdot}$ ions, if the charge and the radical site after electron loss are located on the C-terminal side. As a general statement, the abundance of fragment ions results from both direct fragmentation of the precursor ions and fragmentation of the charge-reduced radical ions obtained after electron loss (EPD). $(y_n-1)^{-\cdot}$ radical ions could also be formed by H elimination from the $(y_n)^-$ ions. Three new $(y_n-2)^-$ ions are detected for this peptide at n=3, 8, and 9 positions and could be formed by H elimination from the $(y_n-1)^{-\cdot}$ ions. The fragmentation of the C-N bond close to the Pro residue can also explain the formation of the $(y_3-2)^-$ fragment ion [14]. Once again, these fragment ions could also arise from the homolytic cleavage of C-N bond fragmentation from the charge-reduced $[M-2H]^{-\cdot}$ radical species. One $(b_8+2)^-$ fragment ion is detected at *m/z* 833.4757 for this peptide due to the presence of the Pro residue [14]. A neutral loss of 44.0264 Da corresponds to C_2H_4O of Thr observed at *m/z* 789.4493 from $(b_8+2)^-$ (**Figure 1A**).

c/z ions are less abundant for this peptide. Two $(c_n)^-$ ions are detected at n=7 and 9 positions. Moreover, two $(c_n-1)^{-\cdot}$ ions at n=9,10 positions and $(c_n-2)^-$ ions at n=7, 10 sites are observed. Radical $(c_n-1)^{-\cdot}$ ions could be produce via the homolytic cleavage of the N-C_α bond from the precursor ion (Scheme 4). Hydrogen abstraction from c ions are also detected in ECD [22, 56, 57]. The formation of the $(c_n-2)^-$ ions could be explained by the radical induced fragmentation of the N-C_α bond from the charge-reduced $[M-2H]^{-\cdot}$ radical species after electron loss.

The Photodissociation of Peptide 2 (DYKDDDDK)

The photodissociation spectrum of the doubly-deprotonated $[M-2H]^{2-}$ (*m/z* 505.1906) of peptide DYKDDDDK is presented in **Figure 3 and S3**. Exact masses and assignments of fragment ions of this peptide are summarized in **Table 3**. Intense neutral losses are also evident from this peptide (**Table S1**). Loss of H_2O from the charge-reduced radical species $[M-2H]^{-\bullet}$ is detected at *m/z* 992.3709. Losses of one, two and three CO_2 are identified at *m/z* 966.3913, 922.4019, and 878.4116, respectively. Madsen *et al* observed one and two CO_2 loss at 193 nm UVPD of singly and multiply charged peptide anions [49]. Abundant CO_2 loss was moreover demonstrated in electron detachment dissociation for peptide and protein [29, 30]. Elimination of several CO_2 is a common feature related to aspartic and glutamic acid residues in NETD, Al-NETD, EDD and UVPD [27, 30]. The UVPD spectrum showed losses of 27.9955 Da from $[M-2H]^{-\bullet}$ that can be attributed to CO, similar to peptide 1. Loss of CO from radical species is also found in an earlier ECD study [58]. The peaks at *m/z* 903.3321 and 904.3394 correspond to the losses of tyrosylate groups of Tyr (107.0491 and 106.0418 Da) from the $[M-2H]^{-\bullet}$. Radical $C_3H_6O_2N$ (88.0371 Da) group elimination from the aspartic amino acid yields to the ion detected at *m/z* 922.3441. The ion observed at *m/z* 938.3961, can be assigned to the loss of $C_3H_4O_2$ (71.9851 Da) from Asp residue [26]. Loss of Lys residue (100.0736 Da) is also detected at *m/z* 910.3076. Moreover, a loss of 71.0713 Da (C_4H_9N) observed for the ion at *m/z* 939.3099 is from the Lys residue [26]. A combined loss of CO_2 and H_2O appears at *m/z* 948.3803.

A complete series of $(a_n)^-$ fragment ion is observed for this peptide for n=2-7. $(a_n+1)^{-\cdot}$ ions are detected for n=4, 5, 6 and 7. These ions are formed via homolytic cleavage from the precursor ion (**Scheme 1**). Radical $(a_n-1)^{-\cdot}$ ions are detected for n= 3, 5 and 6. Fragmentation of the C_α - C bond from the charge-reduced radical species $[M-2H]^{-\bullet}$ is involved to produce these series. Secondary radical elimination of hydrogen atom from $(a_n)^-$ ions could also yield to the formation of these ions. A complete series of $(x_n)^-$ fragment ions is detected at n=2-7 similar to complementary $(a_n)^-$ ions. Two radical $(x_n+1)^{-\cdot}$ ions (n=3 and 6) are detected at *m/z* 402.1380 and 760.2859, respectively. Moreover, two $(x_n+2)^-$ ions (n=2 and 6), which are formed by addition of one extra hydrogen atom to $(x_n+1)^-$ ions are detected. Additionally, $(x_7-1)^-$ ion is observed at *m/z* 921.3364. Same fragmentation mechanisms are proposed for the formation of these ions than for the peptide 1

described previously. A distinctive peaks at *m/z* 886.3281 corresponds to the loss of one and two H_2O molecules from $(x_7)^-$, respectively.

Two $(b_n)^-$ fragment ions are observed at n=1 and 7 sites whereas very abundant radical $(b_n\text{-}1)^{-\cdot}$ ions are detected for n= 1, 3-7. These ions would come from the fragmentation of the C-N bond from the charge-reduced $[M\text{-}2H]^{-\bullet}$ radical species. Several $(y_n)^-$ ions appear at n= 3-6 positions. Some $(y_n\text{-}1)^{-\cdot}$ ions at n=3, 6, 7 sites are also detected (formed via the mechanism proposed **Scheme 3**) as well as $(y_7\text{-}2)^-$ ion. Specific radical induced fragmentation of the $[M\text{-}2H]^{-\bullet}$ radical species is then also observed, after electron loss, for this peptide.

Cleavage of N-C_α bonds produces series of c and z ions. Four $(c_n)^-$ ions and $(c_n\text{-}1)^{-\cdot}$ radical ions are noticed at n=4-7 positions. These ions arise from the homolytic cleavage of the N-C_α bond from the precursor ion (**Scheme 4**). However, complementary $(z_n+1)^{-\cdot}$ radical ions are not detected. $(z_n)^-$ ions are detected from 2, 3, 6 and 7 positions. Interestingly, complete series of radical $(z_n\text{-}1)^{-\cdot}$ ions (n=2-7) is observed for this peptide. Classical fragmentation of the N-C_α bond with proton transfers from the $[M\text{-}2H]^{-\bullet}$ radical species is proposed for the formation of these ions as well as the $(c_n\text{-}1)^{-\cdot}$ series. Compared to first peptide, abundance of c and z ions is noticeable for this peptide and may be due to the presence of five Asp residues. Removal of one H_2O, one CO_2 and combined CO_2 and H_2O from $(z_2)^-$ ion are detected at *m/z* 225.0868 199.1074, and 181.0967, respectively. Previous studies also noticed the losses of H_2O and CO_2 from z ion when peptide contained Asp residues [54]. Combinations of backbone cleavages and neutral losses are listed in **Table S1**.

The Photodissociation of Peptide 3 (RGDSPASSKP)

The photodissociation spectrum of the doubly-deprotonated $[M\text{-}2H]^{2-}$ (*m/z* 499.2393) of peptide RGDSPASSKP is presented in **Figure 4 and S4.** Exact masses and assignments of fragment ions of this peptide are summarized in **Table S2**. Intense neutral losses are summarized in **Table S3**. The loss of H_2O from the charge-reduced radical species $[M\text{-}2H]^{-\bullet}$ (*m/z* 998.4767) is noticed at *m/z* 980.4673 (**Figure 4A**). There are three Ser residues in this peptides and loss of CH_2O (30.0095 Da) at *m/z* 968.4672 can be attributed to the side chain of Ser. The loss of 60.0540 Da observed for the peak at *m/z* 938.4227 corresponds to the C_2H_6ON group of the Ser residue. Loss of CO_2 (exact mass 43.9895 Da) from the carboxyl group located in C-terminal or side chain of aspartic acid

appears at *m/z* 954.4872. Two distinctive peaks at *m/z* 899.3982 and 912.4072 correspond to the losses of 99.0785, and 86.0695 Da from the arginine side chain [26, 53]. Loss of 88.0498 Da which is detected at *m/z* 910.4269 is related to the side chain of Asp [59].

Nearly complete series of $(a_n)^-$ fragment ions is observed for this peptide for n=2-9 whereas $(a_n\text{-}1)^{-\cdot}$ ions are detected for n= 6 and 9. Radical $(a_n+1)^{-\cdot}$ ions are detected for n=2-9 (**Scheme 1**). Addition of one hydrogen to $(a_n+1)^{-\cdot}$ radical ions (similar as shown in **Scheme 2** for the x_n+1 ions) which yield $(a_n+2)^-$ is also prevalent for n=3-5,7-9 positions. $(a_n+2)^-$ ions are also observed for Proline containing peptides [14, 60] and explain the formation of $(a_4+2)^{-\cdot}$ and $(a_9+2)^-$ ions. An almost complete series of $(x_n)^-$ fragment ions is detected at n=1-4, 6-9 similar to the complementary $(a_n)^-$ ions. Four $(x_n\text{-}1)^{-\cdot}$ ions are observed for n= 1, 4, 7-9 sites. Moreover, $(x_n+1)^{-\cdot}$ ions are detected for n=1-4, 6, 7, and 9. Three $(x_n+2)^-$ ions (n=2, 3, 6 and 7) are also formed via H addition on the $(x_n+1)^{-\cdot}$ ions.

$(b_n)^-$ and $(y_n)^-$ fragments ions are predominant in this peptides, which may be due to the presence of basic Arg and Lys amino acids [61]. $(b_n)^-$ ions are identified for n=1-5, 8, and 9 positions only missing n=6 and 7 related to Ala-Ser and Ser-Ser amide bonds. $(b_n+1)^{-\cdot}$ ions are detected for n= 4, 5, and 9 **(Scheme 3)**. Three $(b_n\text{-}1)^{-\cdot}$ ions are observed at n= 3, 8 and 9. Representative $(b_n+2)^-$ ions appear at 2, 4, 9 positions in which two sites (4 and 9) are closed to the Pro residues. $(b_2+2)^-$ ion could be explain by the H addition on the $(b_n+1)^{-\cdot}$ ion. Complete sequence of $(y_n)^-$ ions are found (n= 1-3, 5-9) whereas $(y_n\text{-}1)^{-\cdot}$ ions are noticed for n=2, 5-9. Distinctive $(y_n\text{-}2)^-$ ions are detected for n=1, 2, 6-9.

Homolytic cleavage and fragmentation, associated with proton transfers, of N-C_α bonds is also noticeable. Full sequence of $(c_n)^-$ ions located for n=1-3, 5-9 and $(c_n\text{-}1)^{-\cdot}$ ions are noticed at n= 3, 6-9. Fragment $(c_n\text{-}2)^-$ ions are detected for n= 2, 3, 6-8. Similar to peptide 2, complete series of $(z_n)^-$ ions (n=2-9) are generated from this peptide. $(z_n\text{-}1)^{-\cdot}$ ions are also observed for n=3,7-9. Moreover, $(z_n+1)^{-\cdot}$ ions are detected for n=2, 4, 6, 7 and 9 (**Scheme 4**).

Photo-induced Hydrogen loss at 213 nm

A general trend is observed for those three peptides with series of backbone cleavages leading to ions deficient in hydrogen. All three peptides produce the distinctive doubly-deprotonated $[M\text{-}2H]^-$

$^{\bullet}$ charge-reduced radical species upon irradiation of the monoisotopic precursor ion $[M-2H]^{2-}$, along with hydrogen loss from the charge-reduced radical species as shown in (**Figure 5**). Time-dependent density functional theory (TDDFT) calculation has been performed on a model amide system to elucidate the role of πσ* excited state in the photodissociation of peptide. The potential energy surface of the model amide system, π, π*, and σ* molecular orbitals are displayed in **Figure 6**. The lowest ππ*, πσ* and electronic group state (S_0) are shown with respect to the N-H stretching coordinate of the model amide. The ππ* excitation is observed for the amide system at 215 nm (5.75 eV) which relates with our UVPD experiment at 213 nm. The diffuse and polar character of σ* orbital is observed which is similar to the previous studies on pyrrole/indole system [62, 63]. The shallow barrier with respect to N-H stretch indicates the repulsive nature of this state [62]. For this amide system, the ππ* surface is above the πσ* surface which may allow the fast internal crossing from the ππ* to the πσ* states and lead to H atom dissociation [63-65]. The ππ* excitation-induced amide hydrogen loss then provides a general route for the formation of hydrogen-deficient ions in 213 nm UVPD. Repetition of this mechanism with absorption of several photons can lead to fragments displaying multiple H-loss. Moreover, the ππ* excitation-induced amide hydrogen loss may yield a nitrogen-centered amide anion intermediate and stimulate the wide-spread backbone fragmentation. However, details theoretical calculation are sought to elicit the mechanism of radical-driven side-chain loss and backbone fragmentation at 213 nm photodissociation on peptide and protein anions. Similar mechanism can also arise on other bonds from aromatic cycles or COO chromophore groups.

Conclusion

The key features of these experiments can be summarized as follows: (1) Extensive sequence specific side-chain losses are observed for all three peptides. (2) Near complete series of classical backbone cleavages (a/x, b/y, c/z) are observed. (3) Unusual fragment ions including $(x+1)^{-\cdot}$, $(x+2)^{-}$, $(x-1)^{-\cdot}$, $(y-1)^{-\cdot}$, $(y-2)^{-}$, $(z-1)^{-\cdot}$, $(z+1)^{-\cdot}$, $(z+2)^{-}$ and $(a-1)^{-\cdot}$, $(a+1)^{-\cdot}$, $(a+2)^{-}$, $(b-1)^{-\cdot}$, $(b+1)^{-\cdot}$, $(b+2)^{-}$, $(c-1)^{-\cdot}$, $(c-2)^{-}$ are consistently observed in these experiments and further confirmed by selecting single isotopic peak of the precursor ions. Some of these ions are coming from homolytic cleavages of the backbone from the precursor doubly charged ion. Classical fragmentation of backbone bonds concerted with proton transfers and homolytic cleavages are also observed for the charge-reduced $[M-2H]^{-\cdot}$ radical species after electron photo-detachment. Radical-induced specific fragment ions

are then produced in these experiments of UVPD in the negative mode. Some of these ions may also result from secondary H eliminations. (4) Hydrogen-deficient ions may result from ππ* excitation-induced amide hydrogen loss. This ππ* excitation is reached upon absorption of a photon at 213 nm. The present study outlines the difficulty to interpret and systematically analyze the wealth of fragmentation produced by irradiation of peptide and protein anions at the onset of the amide bond absorption band, which may be different from VUV excitation.

Acknowledgements

The research leading to these results has received funding from the European Research Council under the European Union's Seventh Framework Programme (FP7/2007-2013 Grant agreement N°320659)

Supporting Information: Figures S1-S4 and Table S1-S3 are included in the supporting file.

References:

1. Zhurov, K.O., Fornelli, L., Wodrich, M.D., Laskay, U.A., Tsybin, Y.O.: Principles of electron capture and transfer dissociation mass spectrometry applied to peptide and protein structure analysis. Chem. Soc. Rev. **42**, 5014-5030 (2013)
2. McLuckey, S.A.: Principles of collisional activation in analytical mass spectrometry. J, Am. Soc. Mass Spectrom. **3**, 599-614 (1992)
3. Wells, J. M., McLuckey, S. A.: Collision-induced dissociation (CID) of peptides and proteins. Methods in Enzymol. 402, 148-185 (2005)
4. Zubarev, R.A., Kelleher, N.L., McLafferty, F.W.: Electron capture dissociation of multiply charged protein cations. A nonergodic process. J. Am. Chem. Soc. **120**, 3265-3266 (1998)
5. Syka, J.E.P., Coon, J.J., Schroeder, M.J., Shabanowitz, J., Hunt, D.F.: Peptide and protein sequence analysis by electron transfer dissociation mass spectrometry. Proc Natl Acad Sci USA. **101**, 9528-9533 (2004)
6. Brodbelt, J.S.: Shedding Light on the Frontier of Photodissociation. J. Am. Chem. Soc. **22**, 197-206 (2011)
7. Brodbelt, J.S.: Photodissociation mass spectrometry: new tools for characterization of biological molecules. Chem. Soc. Rev. **43**, 2757-2783 (2014)
8. Antoine, R., Lemoine, J., Dugourd, P.: Electron Photodetachment Dissociation For Structural Characterization Of Synthetic And Bio-Polymer Anions. Mass Spectrom. Rev. **33**, 501-522 (2014)

9. Vasicek, L.A., Ledvina, A.R., Shaw, J., Griep-Raming, J., Westphall, M.S., Coon, J.J., et al.: Implementing Photodissociation in an Orbitrap Mass Spectrometer. J. Am. Soc. Mass Spectrom. **22**, 1105-1108 (2011)
10. Vasicek, L., Brodbelt, J.S.: Enhancement of Ultraviolet Photodissociation Efficiencies through Attachment of Aromatic Chromophores. Anal. Chem. **82**, 9441-9446 (2010)
11. Smith, S.I., Brodbelt, J.S.: Characterization of Oligodeoxynucleotides and Modifications by 193 nm Photodissociation and Electron Photodetachment Dissociation. Anal. Chem. **82**, 7218-7226 (2010)
12. Robinson, M.R., Madsen, J.A., Brodbelt, J.S.: 193 nm Ultraviolet Photodissociation of Imidazolinylated Lys-N Peptides for De Novo Sequencing. Anal. Chem. **84**, 2433-2439 (2012)
13. Tabarin, T., Antoine, R., Broyer, M., Dugourd, P.: Specific photodissociation of peptides with multi-stage mass spectrometry. Rapid Comm. Mass Spectrom. **19**, 2883-2892 (2005)
14. Girod, M., Zeljka, S., Marin, V., Rodolphe, A., Luke, M., J., L., et al.: UV Photodissociation of Proline-containing Peptide Ions: Insights from Molecular Dynamics. J. Am. Soc. Mass Spectrom. **26**, 432--443 (2014)
15. Shaw, J.B., Li, W.Z., Holden, D.D., Zhang, Y., Griep-Raming, J., Fellers, R.T., et al.: Complete Protein Characterization Using Top-Down Mass Spectrometry and Ultraviolet Photodissociation. J. Am. Chem. Soc. **135**, 12646-12651 (2013)
16. Cannon, J.R., Carnmarata, M.B., Robotham, S.A., Cotham, V.C., Shaw, J.B., Fellers, R.T., et al.: Ultraviolet Photodissociation for Characterization of Whole Proteins on a Chromatographic Time Scale. Anal. Chem. **86**, 2185-2192 (2014)
17. Madsen, J., Cheng, R.R., Kaoud, T.S., Dalby, K.N., Makarov, D.E., Brodbelt, J.S.: Charge-site-dependent dissociation of hydrogen-rich radical peptide cations upon vacuum UV photoexcitation. Chem. Eur. J. **18**, 5374--5383 (2012)
18. Thompson, M.S., Weidong, C., P., Reilly .J.P.: Fragmentation of singly charged peptide ions by photodissociation at lamda = 157 nm. Angew. Chem. Int. Ed. **43**, 4791--4794 (2004)
19. Cui, W., Thompson, M.S., Reilly, J.P.: Pathways of peptide ion fragmentation induced by vacuum ultraviolet light. J. Am. Soc. Mass Spectrom. **16**, 1384--1398 (2005)
20. Zhang, L., Cui, W., Thompson, M.S., Reilly, J.P.: Structures of α-Type Ions Formed in the 157 nm Photodissociation of Singly-Charged Peptide Ions. J. Am. Soc. Mass Spectrom. **17**, 1315-1321 (2006)
21. Kim, T.-Y., Reilly, J.P.: Time-Resolved Observation of Product Ions Generated by 157 nm Photodissociation of Singly Protonated Phosphopeptides. J. Am. Soc. Mass Spectrom. **20**, 2334-2341 (2009)
22. Zubarev, R.A., Horn, D.M., Fridriksson, E.K., Kelleher, N.L., Kruger, N.A., Lewis, M.A., et al.: Electron Capture Dissociation for Structural Characterization of Multiply Charged Protein Cations. Anal. Chem. **72**, 563-573 (2000)
23. O'Connor, P.B., Lin, C., Cournoyer, J.J., Pittman, J.L., Belyayev, M., Budnik, B.A.: Long-Lived Electron Capture Dissociation Product Ions Experience Radical Migration via Hydrogen Abstraction. J. Am. Soc. Mass Spectrom. **17**, 576-585 (2006)
24. Kjeldsen, F., Silivra, O.A., Ivonin, I.A., Haselmann, K.F., Gorshkov, M., Zubarev, R.A.: Cα□ C Backbone Fragmentation Dominates in Electron Detachment Dissociation of Gas-Phase Polypeptide Polyanions. Chem. Eur. J. **11**, 1803-1812 (2005)

25. Shaw, J.B., Madsen, J., Xu, H., Brodbelt, J.S.: Systematic comparison of ultraviolet photodissociation and electron transfer dissociation for peptide anion characterization. J. Am. Soc. Mass Spectrom. **23**, 1707--1715 (2012)
26. Rumachik, N.G., McAlister, G.C., Russell, J.D., Bailey, D.J., Wenger , C.D., Coon, J.J.: Characterizing peptide neutral losses induced by negative electron-transfer dissociation (NETD). J. Am. Soc. Mass Spectrom. **23**, 718--727 (2012)
27. Shaw, J.B., Kaplan, D.A., Brodbelt, J.S.: Activated Ion Negative Electron Transfer Dissociation of Multiply Charged Peptide Anions. Anal. Chem. **85**, 4721-4728 (2013)
28. Larraillet, V., Vorobyev, A., Brunet, C., Lemoine, J., Tsybin, Y.O., Antoine, R., et al.: Comparative Dissociation of Peptide Polyanions by Electron Impact and Photo-Induced Electron Detachment. J. Am. Soc. Mass Spectrom. **21**, 670-680 (2010)
29. Larraillet, V., Antoine, R., Dugourd, P., J., L., me: Activated-electron photodetachment dissociation for the structural characterization of protein polyanions. Anal. Chem. **81**, 8410--8416 (2009)
30. Antoine, R., Joly, L., Tabarin, T., Broyer, M., Dugourd, P., Lemoine, J.: Photo-induced formation of radical anion peptides. Electron photodetachment dissociation experiments. Rapid Comm. Mass Spectrom. **21**, 265-268 (2007)
31. Ganisl, B., Valovka, T., Hartl, M., Taucher, M., Bister, K., Breuker, K.: Electron Detachment Dissociation for Top-Down Mass Spectrometry of Acidic Proteins. Chem. Eur. J. **17**, 4460-4469 (2011)
32. Turecek, F., Julian, R.R.: Peptide Radicals and Cation Radicals in the Gas Phase. Chem. Rev. **113**, 6691-6733 (2013)
33. Moore, B.N., Ly, T., Julian, R.R.: Radical Conversion and Migration in Electron Capture Dissociation. J. Am. Chem. Soc. **133**, 6997-7006 (2011)
34. Zubarev, R.: Peptide radical cations: gender determines dissociation chemistry. Mass spectrom. (Tokyo, Japan). **2**, S0004-S0004 (2013)
35. Coon, J.J., Shabanowitz, J., Hunt, D.F., Syka, J.E.P.: Electron Transfer Dissociation of Peptide Anions. J. Am. Soc. Mass Spectrom. **16**, 880-882 (2005)
36. Oh, H.B., Moon, B.: Radical-Driven Peptide Backbone Dissociation Tandem Mass Spectrometry. Mass Spectrom. Rev. **34**, 116-132 (2015)
37. Sohn, C.H., Chung, C.K., Yin, S., Ramachandran, P., Loo, J.A., Beauchamp, J.L.: Probing the Mechanism of Electron Capture and Electron Transfer Dissociation Using Tags with Variable Electron Affinity. J. Am. Chem. Soc. **131**, 5444-5459 (2009)
38. Kalli, A., Hess, S.: Electron Capture Dissociation of Hydrogen-Deficient Peptide Radical Cations. J. Am. Soc. Mass Spectrom. **23**, 1729-1740 (2012)
39. Sun, Q., Nelson, H., Ly, T., Stoltz, B.M., Julian, R.R.: Side Chain Chemistry Mediates Backbone Fragmentation in Hydrogen Deficient Peptide Radicals. J. Proteom. Res. **8**, 958-966 (2009)
40. Patiny, L., Borel, A.: ChemCalc: A Building Block for Tomorrow's Chemical Infrastructure. J. Chem. Inf. Model. **53**, 1223-1228 (2013)
41. Frisch, M., Trucks, G., Schlegel, H.B., Scuseria, G., Robb, M., Cheeseman, J., et al.: Gaussian 09, Revision A. 02, Gaussian. Inc., Wallingford, CT. **200**, (2009)
42. Becke, A.D.: Density-functional exchange-energy approximation with correct asymptotic behavior. Phys. Rev. A. **38**, 3098 (1988)
43. Lee, C., Yang, W., Parr, R.G.: Development of the Colle-Salvetti correlation-energy formula into a functional of the electron density. Phys. Rev. B. **37**, 785 (1988)

44. Reed, A.E., Weinstock, R.B., Weinhold, F.: Natural population analysis. J. Chem. Phys. **83**, 735-746 (1985)
45. Reed, A.E., Curtiss, L.A., Weinhold, F.: Intermolecular interactions from a natural bond orbital, donor-acceptor viewpoint. Chem. Rev. **88**, 899-926 (1988)
46. Runge, E., Gross, E.K.: Density-functional theory for time-dependent systems. Phys. Rev. Lett. **52**, 997 (1984)
47. Han, X., Jin, M., Breuker, K., McLafferty, F.W.: Extending Top-Down Mass Spectrometry to Proteins with Masses Greater Than 200 Kilodaltons. Science. **314**, 109-112 (2006)
48. Yoo, H.J., Ning, W., Shuyi, Z., Hangtian, S., Kristina, H.: Negative-ion electron capture dissociation: Radical-driven fragmentation of charge-increased gaseous peptide anions. J. Am. Chem. Soc. **133**, 16790--16793 (2011)
49. Madsen, J., Kaoud, T.S., Dalby, K.N., Brodbelt, J.S.: 193-Nm Photodissociation of Singly and Multiply Charged Peptide Anions for Acidic Proteome Characterization. Proteom. **11**, 1329--1334 (2011)
50. Bowie, J.H., Brinkworth, C.S., Dua, S.: Collision-induced fragmentations of the (M-H)− parent anions of underivatized peptides: An aid to structure determination and some unusual negative ion cleavages. Mass Spectrom. Rev. **21**, 87-107 (2002)
51. Han, H., Xia, Y., McLuckey, S.A.: Ion Trap Collisional Activation of c and z• Ions Formed via Gas-Phase Ion/Ion Electron-Transfer Dissociation. J. Proteom. Res. **6**, 3062-3069 (2007)
52. Zhang, L., Reilly, J.P.: Radical-Driven Dissociation of Odd-Electron Peptide Radical Ions Produced in 157 nm Photodissociation. J. Am. Soc. Mass Spectrom. **20**, 1378-1390 (2009)
53. Papayannopoulos, I.A.: The interpretation of collision-induced dissociation tandem mass spectra of peptides. Mass Spectrom. Rev. **14**, 49-73 (1995)
54. Chu, I. K., Siu, C. K., Lau, J. K. C., Tang, W. K., Mu, X., Lai, C. K., et al.: Proposed nomenclature for peptide ion fragmentation. Int. J. Mass Spectrom. (In press) doi:10.1016/j.ijms.2015.07.021 (2015).
55. Madsen, J. A., Xu, H., Robinson, M. R., Horton, A. P., Shaw, J. B., Giles, D. K., et al.: High-throughput database search and large-scale negative polarity liquid chromatography–tandem mass spectrometry with ultraviolet photodissociation for complex proteomic samples. Mol. Cell. Proteom. **12**, 2604-2614 (2013).
56. Fung, Y.M.E., Dominic, C.T.W.: Experimental and theoretical investigations of the loss of amino acid side chains in electron capture dissociation of model peptides. J. Am. Soc. Mass Spectrom. **16**, 1523--1535 (2005)
57. Tureček, F., Syrstad, E.A.: Mechanism and Energetics of Intramolecular Hydrogen Transfer in Amide and Peptide Radicals and Cation-Radicals. J. Am. Chem. Soc. **125**, 3353-3369 (2003)
58. Cooper, H.J., Hudgins, R.R., Håkansson, K., Marshall, A.G.: Characterization of amino acid side chain losses in electron capture dissociation. J. Am. Soc. Mass Spectrom. **13**, 241-249 (2002)
59. Harrison, A.G., Tu, Y.P.: Ion chemistry of protonated aspartic acid derivatives. J. Mass Spectrom. **33**, 532-542 (1998)

60. Kim, T.-Y., Valentine, S.J., Clemmer, D.E., Reilly, J.P.: Gas-Phase Conformation-Specific Photofragmentation of Proline-Containing Peptide Ions. J. Am. Soc. Mass Spectrom. **21**, 1455-1465 (2010)
61. Summerfield, S.G., Whiting, A., Gaskell, S.J.: Intra-ionic interactions in electrosprayed peptide ions. Int. J. Mass. Spectrom. Ion Processes. **162**, 149-161 (1997)
62. Sobolewski, A.L., Domcke, W., Dedonder-Lardeux, C., Jouvet, C.: Excited-state hydrogen detachment and hydrogen transfer driven by repulsive (1)pi sigma* states: A new paradigm for nonradiative decay in aromatic biomolecules. Phys. Chem. Chem. Phys. **4**, 1093-1100 (2002)
63. Ashfold, M.N.R., King, G.A., Murdock, D., Nix, M.G.D., Oliver, T.A.A., Sage, A.G.: pi sigma* excited states in molecular photochemistry. Phys. Chem. Chem. Phys. **12**, 1218-1238 (2010)
64. Ashfold, M.N.R., Cronin, B., Devine, A.L., Dixon, R.N., Nix, M.G.D.: The role of pi sigma* excited states in the photodissociation of heteroaromatic molecules. Science. **312**, 1637-1640 (2006)
65. Sage, A.G., Nix, M.G.D., Ashfold, M.N.R.: UV photodissociation of N-methylpyrrole: The role of pi sigma* states in non-hydride heteroaromatic systems. Chem. Phys. **347**, 300-308 (2008)

Tables and Figures

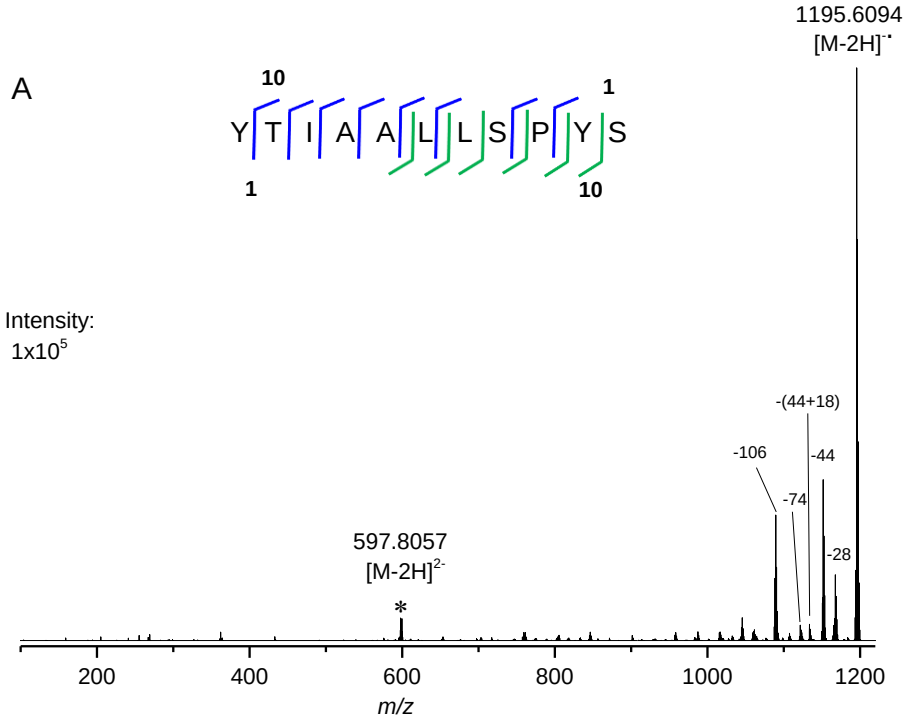

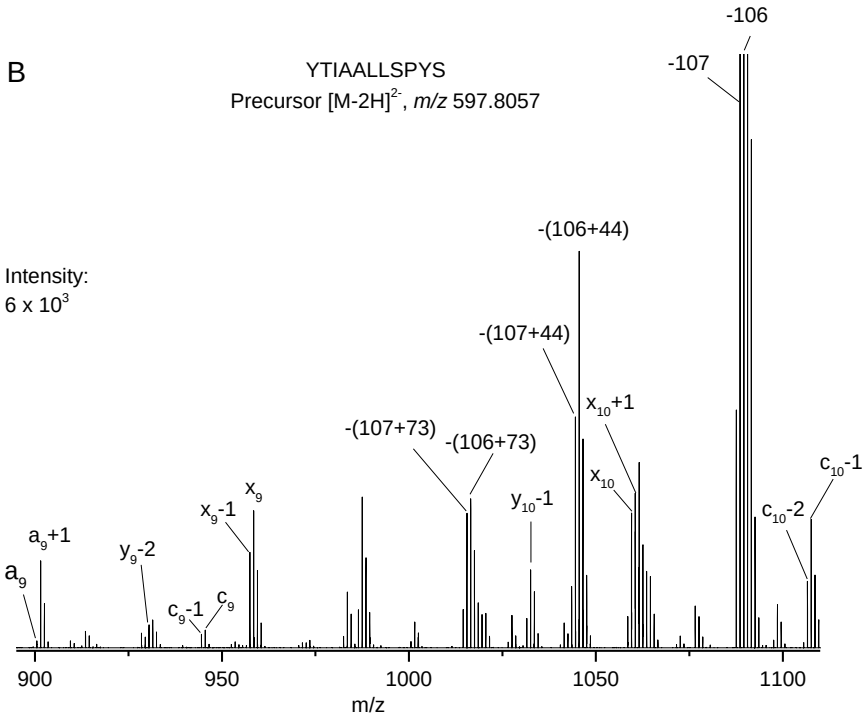

C

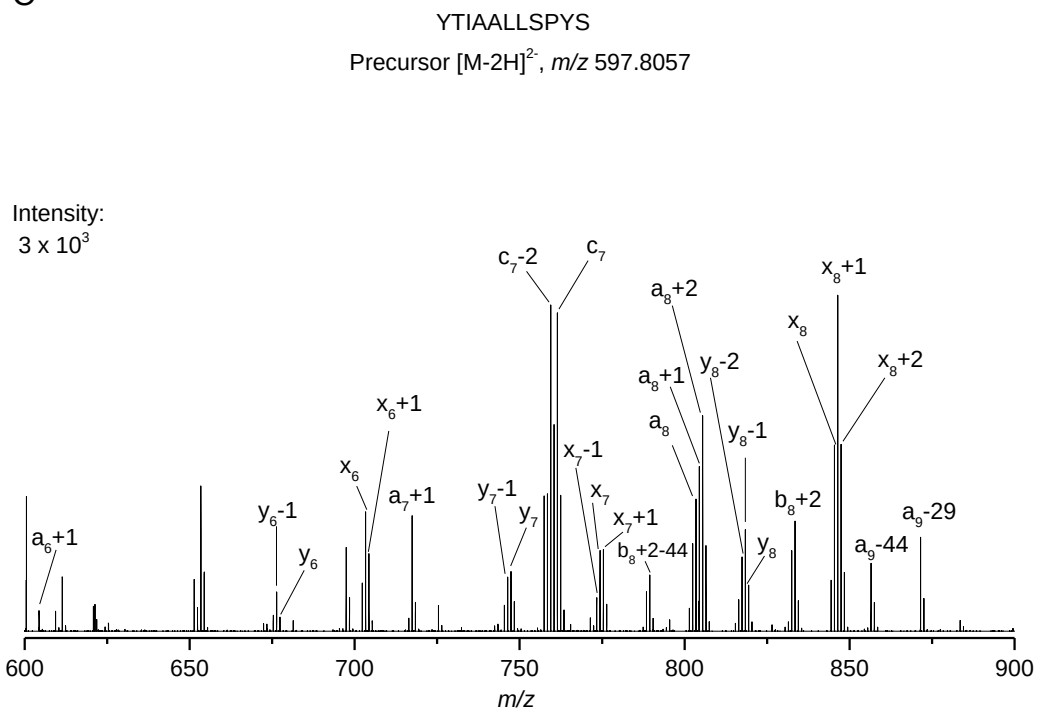

Figure 1. Photodissociation spectra of the doubly-deprotonated $[M-2H]^{2-}$ ion (*m/z*=597.8057) of YTIAALLSPYS at 213 nm. The precursor ion is notified by * sign and the neutral losses are indicated by ion masses. The green and blue lines represent the a, b, c and x, y, z ions, respectively. A) Spectrum of 100-1200 *m/z*, B) Spectrum of 900-1100 *m/z*, and C) Spectrum of 600-900 *m/z*.

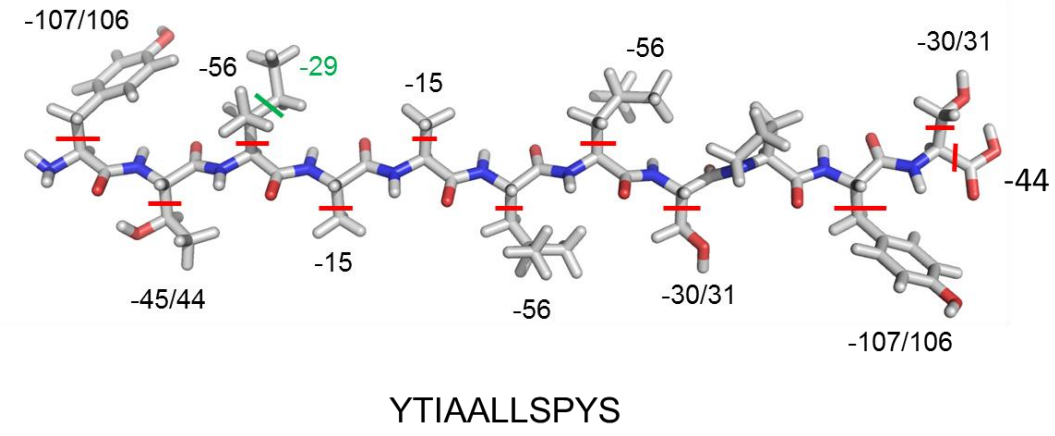

Figure 2. Side-chain losses detected from peptide 1, YTIAALLSPYS at 213 nm.

Table 1. Exact masses and assignments of ions from backbone dissociation detected in the UVPD of doubly-deprotonated (*m/z*=597.8057) of YTIAALLSPYS $[M-2H]^{2-}$.

Experimental *m/z*	Theoretical *m/z*	Assignment	Chemical Composition	Mass Difference (ppm)
267.0977	267.0981	$(y_2)^-$	$C_{12}H_{15}N_2O_5$	-0.1721
294.0848	294.0852	$(x_2+1)^{-\cdot}$	$C_{13}H_{14}N_2O_6$	-0.1477
295.0924	295.0852	$(x_2+2)^-$	$C_{13}H_{15}N_2O_6$	2.9264
362.1348	362.1352	$(y_3-2)^-$	$C_{17}H_{20}N_3O_6$	-0.1696
364.1505	364.1509	$(y_3)^-$	$C_{17}H_{22}N_3O_6$	-0.1575
491.2612	491.2744	$(a_5+1)^{-\cdot}$	$C_{24}H_{37}N_5O_6$	-5.3107
591.2533	591.2540	$(x_5+1)^{-\cdot}$	$C_{27}H_{37}N_5O_{10}$	-0.2914
604.3579	604.3586	$(a_6+1)^{-\cdot}$	$C_{30}H_{48}N_6O_7$	-0.2089
676.3437	676.3432	$(y_6-1)^{-\cdot}$	$C_{32}H_{48}N_6O_{10}$	0.1889
677.3503	677.3510	$(y_6)^-$	$C_{32}H_{49}N_6O_{10}$	-0.2864
703.3294	703.3303	$(x_6)^-$	$C_{33}H_{47}N_6O_{11}$	-0.3636
704.3384	704.3381	$(x_6+1)^{-\cdot}$	$C_{33}H_{48}N_6O_{11}$	0.1069
717.4287	717.4425	$(a_7+1)^{-\cdot}$	$C_{36}H_{59}N_7O_8$	-5.5519
747.3786	747.3803	$(y_7-1)^{-\cdot}$	$C_{35}H_{54}N_7O_{11}$	-0.6880
748.3876	748.3881	$(y_7)^-$	$C_{35}H_{55}N_7O_{11}$	-0.2259
759.4406	759.4405	$(c_7-2)^-$	$C_{37}H_{59}N_8O_9$	0.0404
761.4556	761.4561	$(c_7)^-$	$C_{37}H_{61}N_8O_9$	-0.2059
773.3587	773.3596	$(x_7-1)^{-\cdot}$	$C_{36}H_{51}N_7O_{12}$	-0.3591
774.3659	774.3674	$(x_7)^-$	$C_{36}H_{52}N_7O_{12}$	-0.5911
775.3733	775.3752	$(x_7+1)^{-\cdot}$	$C_{36}H_{53}N_7O_{12}$	-0.7867
803.4658	803.4667	$(a_8)^-$	$C_{39}H_{63}N_8O_{10}$	-0.3571
804.4737	804.4745	$(a_8+1)^{-\cdot}$	$C_{39}H_{64}N_8O_{10}$	-0.3470
805.4815	805.4824	$(a_8+2)^-$	$C_{39}H_{65}N_8O_{10}$	-0.3612
817.4079	817.4096	$(y_8-2)^-$	$C_{38}H_{57}N_8O_{12}$	-0.6472
818.4158	818.4174	$(y_8-1)^{-\cdot}$	$C_{38}H_{58}N_8O_{12}$	-0.6331
819.4256	819.4252	$(y_8)^-$	$C_{38}H_{59}N_8O_{12}$	0.1435
833.4757	833.4773	$(b_8+2)^-$	$C_{40}H_{65}N_8O_{11}$	-0.6535
845.4032	845.4045	$(x_8)^-$	$C_{39}H_{57}N_8O_{13}$	-0.5119
846.4109	846.4123	$(x_8+1)^{-\cdot}$	$C_{39}H_{58}N_8O_{13}$	-0.5866

847.4204	847.4201	$(x_8+2)^-$	$C_{39}H_{59}N_8O_{13}$	0.1174
900.5049	900.5195	$(a_9)^-$	$C_{44}H_{70}N_9O_{11}$	-5.8453
901.5120	901.5273	$(a_9+1)^{-\cdot}$	$C_{44}H_{71}N_9O_{11}$	-6.1741
930.4916	930.4937	$(y_9-2)^-$	$C_{44}H_{69}N_9O_{13}$	-0.8223
944.5335	944.5331	$(c_9-1)^{-\cdot}$	$C_{45}H_{72}N_{10}O_{12}$	0.1744
945.5378	945.5409	$(c_9)^-$	$C_{45}H_{73}N_{10}O_{12}$	-1.2759
957.4795	957.4807	$(x_9-1)^{-\cdot}$	$C_{45}H_{67}N_9O_{14}$	-0.4833
958.4859	958.4886	$(x_9)^-$	$C_{45}H_{68}N_9O_{14}$	-1.0864
1032.5470	1032.5492	$(y_{10}-1)^{-\cdot}$	$C_{48}H_{76}N_{10}O_{15}$	-0.8721
1059.5334	1059.5440	$(x_{10})^-$	$C_{49}H_{75}N_{10}O_{16}$	-4.2870
1060.5395	1060.5440	$(x_{10}+1)^{-\cdot}$	$C_{49}H_{76}N_{10}O_{16}$	-1.8463
1106.5866	1106.5886	$(c_{10}-2)^-$	$C_{54}H_{80}N_{11}O_{14}$	-0.8114
1107.5938	1107.5964	$(c_{10}-1)^{-\cdot}$	$C_{54}H_{81}N_{11}O_{14}$	-1.0757

Table 2. Exact masses and assignments of neutral loss detected in the UVPD of doubly-deprotonated (*m/z*=597.8057) of YTIAALLSPYS $[M-2H]^{2-}$.

Experimental *m/z*	Theoretical *m/z*	Assignment	Chemical Composition	Mass Difference(ppm)
1195.6094	1195.6119	$[M-2H]^{-\bullet}$	$C_{57}H_{85}N_{11}O_{17}$	-1.0065
1180.5852	1180.5885	$[M-2H-CH_3]^-$	$C_{56}H_{82}N_{11}O_{17}$	-1.3313
1167.6147	1167.6170	$[M-2H-CO]^{-\bullet}$	$C_{56}H_{85}N_{11}O_{16}$	-0.9306
1166.6099	1166.5728	$[M-2H-CH_3CH_2]^-$	$C_{55}H_{80}N_{11}O_{17}$	14.9551
1165.6009	1165.6047	$[M-2H-CH_2O]^{-\bullet}$	$C_{56}H_{83}N_{11}O_{16}$	-1.5532
1164.5942	1164.5935	$[M-2H-CH_2OH]^-$	$C_{56}H_{82}N_{11}O_{16}$	0.2703
1151.5829	1151.6221	$[M-2H-C_2H_4O]^{-\bullet}$	$C_{55}H_{81}N_{11}O_{16}$	-15.7951
1150.5783	1150.6143	$[M-2H-COOH]^-$	$C_{56}H_{84}N_{11}O_{15}$	-14.5355
1139.5855	1139.5504	$[M-2H-C_4H_8]^{-\bullet}$	$C_{53}H_{78}N_{11}O_{17}$	14.1289
1133.6099	1133.6116	$[M-2H-(CO_2+H_2O)]^{-\bullet}$	$C_{56}H_{83}N_{11}O_{14}$	-0.6445
1123.5910	1123.5312	$[M-2H-C_4H_{11}N]^{-\bullet}$	$C_{53}H_{75}N_{10}O_{17}$	24.1551
1121.5759	1121.5513	$[M-2H-(C_3H_8ON)]^-$	$C_{54}H_{77}N_{10}O_{16}$	9.9354
1089.5688	1089.5712	$[M-2H-(OC_6OH_4=CH_2)]^{-\bullet}$	$C_{50}H_{79}N_{11}O_{16}$	-0.9454
1088.5622	1088.5633	$[M-2H-(HOC_6H_4=CH_2)]^-$	$C_{51}H_{78}N_{11}O_{16}$	-0.4512
1045.5419	1045.5449	$[M-2H-(OC_6OH_4=CH_2+C_2H_4O)]^{-\bullet}$	$C_{48}H_{75}N_{11}O_{15}$	-1.2420
1044.5346	1044.5371	$[M-2H-(HOC_6H_4=CH_2+C_2H_4O)\ ]^{-\bullet}$	$C_{48}H_{74}N_{11}O_{15}$	-1.0060
987.5129	987.5271	$[z_{10}-CHO]^{-\bullet}$	$C_{47}H_{73}N_9O_{14}$	-5.7445
986.5053	986.5193	$[z_{10}-1-CHO]^-$	$C_{47}H_{72}N_9O_{14}$	-5.6699
871.5031	871.5162	$[a_9-CH_3CH_2]^{-\bullet}$	$C_{43}H_{69}N_9O_{10}$	-5.2771
856.4917	856.5291	$[a_9-C_2H_4O]^-$	$C_{43}H_{70}N_9O_9$	-15.0806
789.4493	789.4869	$[b_8+2-C_2H_4O]^-$	$C_{39}H_{65}N_8O_9$	-15.1617
597.8057	597.8059	$[M-2H]^{2-}$	$C_{57}H_{85}N_{11}O_{17}$	-0.1139
575.7925	575.8111	$[M-2H-CO_2]^{2-}$	$C_{56}H_{85}N_{11}O_{15}$	-7.4861
205.0700	205.0972	$[y_2-CO_2+H_2O]^-$	$C_{11}H_{13}N_2O_2$	-10.9548

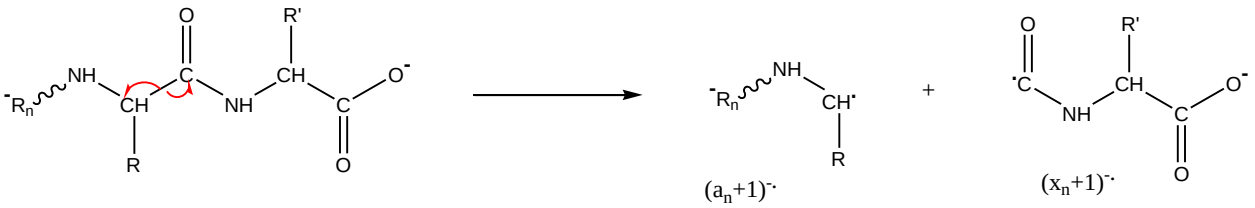

Scheme 1: Proposed mechanism for the formation of $(a_n+1)^{-\cdot}$ and $(x_n+1)^{-\cdot}$ fragment ions during UVPD of doubly deprotonated peptide $[M-2H]^{2-}$.

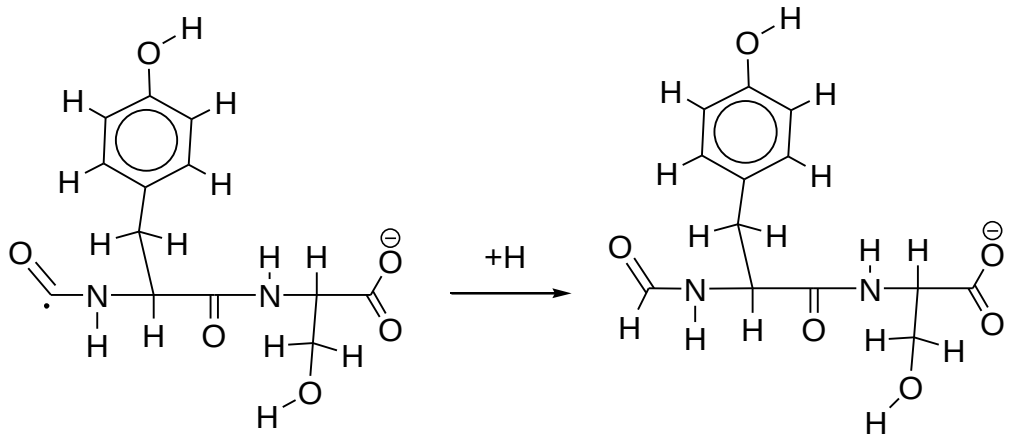

Scheme 2: Proposed mechanism for the formation of $(x_2+2)^{-}$ product ion from the $(x_1+1)^{-\cdot}$ fragment ions during the UVPD of the doubly deprotonated YTIAALLSPYS peptide.

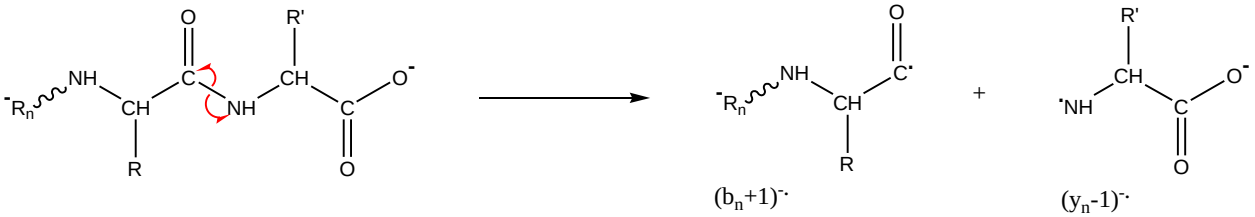

Scheme 3: Proposed mechanism for the formation of $(b_n+1)^{-\cdot}$ and $(y_n-1)^{-\cdot}$ fragment ions during UVPD of doubly deprotonated peptide $[M-2H]^{2-}$.

Scheme 4: Proposed mechanism for the formation of $(c_n\text{-}1)^{-\cdot}$ and $(z_n\text{+}1)^{-\cdot}$ fragment ions during UVPD of doubly deprotonated peptide $[M\text{-}2H]^{2-}$.

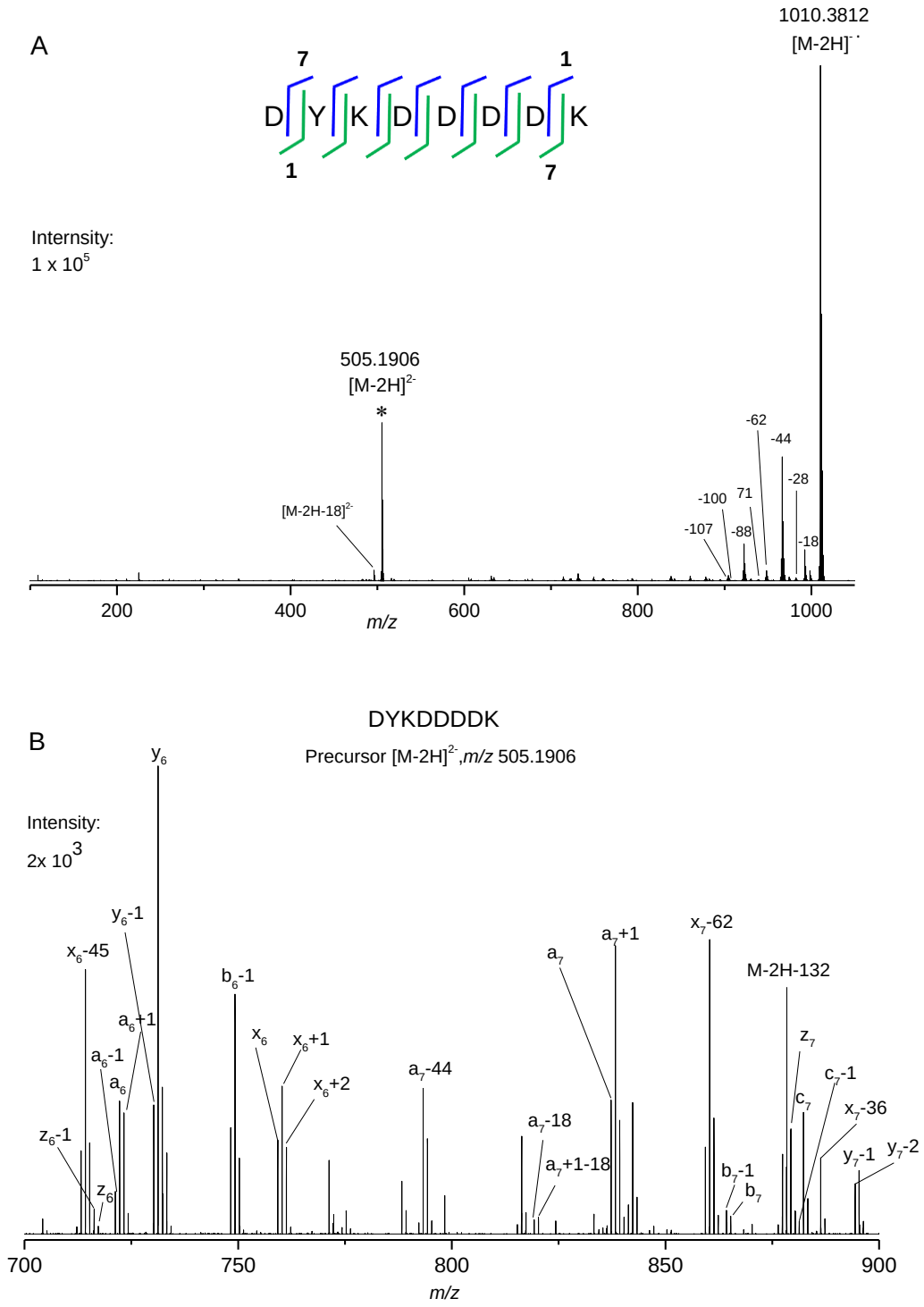

Figure 3. Photodissociation spectra of the doubly-deprotonated $[M-2H]^{2-}$ ion (*m/z*=505.1906) of DYKDDDDK at 213 nm (the precursor ion is signified by * and neutral losses are indicated by ion masses). The green and blue lines represent the a, b, c and x, y, z ions, respectively.

Table 3. Exact masses and assignments of ions from backbone dissociation detected in the UVPD of doubly-deprotonated (*m/z*=505.1906) of DYKDDDDK $[M-2H]^{2-}$.

Experimental *m/z*	Theoretical *m/z*	Assignment	Chemical Composition	Mass Difference(ppm)
113.0339	113.0113	$(b_1\text{-}1)^{-\cdot}$	$C_4H_3NO_3$	9.1566
114.0179	114.0191	$(b_1)^-$	$C_4H_4NO_3$	-0.4551
242.1134	242.0903	$(z_2\text{-}1)^{-\cdot}$	$C_{10}H_{14}N_2O_5$	9.3508
243.0975	243.0981	$(z_2)^-$	$C_{10}H_{15}N_2O_5$	-0.2527
249.0869	249.0875	$(a_2)^-$	$C_{12}H_{13}N_2O_4$	-0.2630
251.0926	251.1032	$(a_2+2)^-$	$C_{12}H_{14}N_2O_4$	-4.2771
286.1034	286.1039	$(x_2)^-$	$C_{11}H_{16}N_3O_6$	-0.2139
288.1197	288.1196	$(x_2+2)^-$	$C_{11}H_{18}N_3O_6$	0.0724
357.1405	357.1172	$(z_3\text{-}1)^{-\cdot}$	$C_{14}H_{19}N_3O_8$	9.3899
358.1252	358.1250	$(z_3)^-$	$C_{14}H_{18}N_3O_8$	0.0647
374.1324	374.1438	$(y_3\text{-}1)^{-\cdot}$	$C_{14}H_{22}N_4O_8$	-4.5965
375.1509	375.1516	$(y_3)^-$	$C_{14}H_{23}N_4O_8$	-0.2818
376.1976	376.1747	$(a_3\text{-}1)^{-\cdot}$	$C_{18}H_{24}N_4O_5$	9.2708
377.1818	377.1825	$(a_3)^-$	$C_{18}H_{25}N_4O_5$	-0.2723
401.1300	401.1309	$(x_3)^-$	$C_{15}H_{21}N_4O_9$	-0.3442
402.1380	402.1387	$(x_3+1)^{-\cdot}$	$C_{15}H_{22}N_4O_9$	-0.2656
404.1926	404.1696	$(b_3\text{-}1)^{-\cdot}$	$C_{19}H_{24}N_4O_6$	9.2932
471.1592	471.1363	$(z_4\text{-}2)^-$	$C_{18}H_{23}N_4O_{11}$	9.2294
472.1673	472.1442	$(z_4\text{-}1)^{-\cdot}$	$C_{18}H_{24}N_4O_{11}$	9.3202
490.1778	490.1785	$(y_4)^-$	$C_{18}H_{28}N_5O_{11}$	-0.3057
491.1933	491.1864	$(y_4+1)^{-\cdot}$	$C_{18}H_{29}N_5O_{11}$	2.7890
492.1965	492.2094	$(a_4)^-$	$C_{22}H_{30}N_5O_8$	-5.2316
493.2165	493.2173	$(a_4+1)^{-\cdot}$	$C_{22}H_{31}N_5O_8$	-0.3199
516.1568	516.1578	$(x_4)^-$	$C_{19}H_{26}N_5O_{12}$	-0.3898
519.2194	519.2043	$(b_4\text{-}1)^{-\cdot}$	$C_{23}H_{29}N_5O_9$	6.0706
536.2224	536.2231	$(c_4\text{-}1)^{-\cdot}$	$C_{23}H_{32}N_6O_9$	-0.2609
537.2301	537.2309	$(c_4)^-$	$C_{23}H_{33}N_6O_9$	-0.3274
587.1941	587.1711	$(z_5\text{-}1)^{-\cdot}$	$C_{22}H_{30}N_5O_{14}$	9.2746
605.2049	605.2055	$(y_5)^-$	$C_{22}H_{33}N_6O_{14}$	-0.2439
606.2282	606.2287	$(a_5\text{-}1)^{-\cdot}$	$C_{26}H_{34}N_6O_{11}$	-0.1597
607.2356	607.2364	$(a_5)^-$	$C_{26}H_{35}N_6O_{11}$	-0.3272

608.2435	608.2442	$(a_5+1)^{-\cdot}$	$C_{26}H_{36}N_6O_{11}$	-0.2848
631.1839	631.1847	$(x_5)^-$	$C_{23}H_{31}N_6O_{15}$	-0.3064
634.2464	634.2235	$(b_5-1)^{-\cdot}$	$C_{27}H_{34}N_6O_{12}$	9.2706
651.2492	651.2500	$(c_5-1)^{-\cdot}$	$C_{27}H_{37}N_7O_{12}$	-0.3387
652.2569	652.2578	$(c_5)^-$	$C_{27}H_{38}N_7O_{12}$	-0.3569
715.2885	715.2661	$(z_6-1)^{-\cdot}$	$C_{28}H_{41}N_7O_{15}$	9.0636
716.2965	716.2739	$(z_6)^-$	$C_{28}H_{42}N_7O_{15}$	9.1301
721.2544	721.2555	$(a_6-1)^{-\cdot}$	$C_{30}H_{39}N_7O_{14}$	-0.4393
722.2624	722.2633	$(a_6)^-$	$C_{30}H_{40}N_7O_{14}$	-0.3728
723.2722	723.2711	$(a_6+1)^{-\cdot}$	$C_{30}H_{41}N_7O_{14}$	0.4320
732.2915	732.2926	$(y_6-1)^{-\cdot}$	$C_{28}H_{44}N_8O_{15}$	-0.4529
733.29893	733.3004	$(y_6)^-$	$C_{28}H_{45}N_8O_{15}$	-0.6083
749.2729	749.2504	$(b_6-1)^{-\cdot}$	$C_{31}H_{39}N_7O_{15}$	9.0999
759.2785	759.2797	$(x_6)^-$	$C_{29}H_{43}N_8O_{16}$	-0.4891
760.2859	760.2875	$(x_6+1)^{-\cdot}$	$C_{29}H_{44}N_8O_{16}$	-0.6767
761.2953	761.2953	$(x_6+2)^-$	$C_{29}H_{45}N_8O_{16}$	-0.0009
766.2783	766.2769	$(c_6-1)^{-\cdot}$	$C_{31}H_{42}N_8O_{15}$	0.5476
767.2834	767.2848	$(c_6)^-$	$C_{31}H_{43}N_8O_{15}$	-0.5397
837.2890	837.2903	$(a_7)^-$	$C_{34}H_{45}N_8O_{17}$	-0.4950
838.2963	838.2980	$(a_7+1)^{-\cdot}$	$C_{34}H_{46}N_8O_{17}$	-0.7068
864.2765	864.2774	$(b_7-1)^{-\cdot}$	$C_{35}H_{44}N_8O_{18}$	-0.3536
865.2866	865.2852	$(b_7)^-$	$C_{35}H_{45}N_8O_{18}$	0.5561
878.3293	878.3294	$(z_7-1)^{-\cdot}$	$C_{37}H_{50}N_8O_{17}$	-0.0574
879.3587	879.3372	$(z_7)^-$	$C_{37}H_{51}N_8O_{17}$	8.6466
881.3027	881.3039	$(c_7-1)^{-\cdot}$	$C_{35}H_{49}N_9O_{18}$	-0.4783
882.3102	882.3117	$(c_7)^-$	$C_{35}H_{48}N_9O_{18}$	-0.6175
894.3471	894.3481	$(y_7-2)^-$	$C_{37}H_{54}N_9O_{17}$	-0.4140
895.3538	895.3559	$(y_7-1)^{-\cdot}$	$C_{37}H_{53}N_9O_{17}$	-0.8800
921.3364	921.3352	$(x_7-1)^{-\cdot}$	$C_{38}H_{51}N_9O_{18}$	0.4656
922.3421	922.3430	$(x_7)^-$	$C_{38}H_{52}N_9O_{18}$	-0.3594

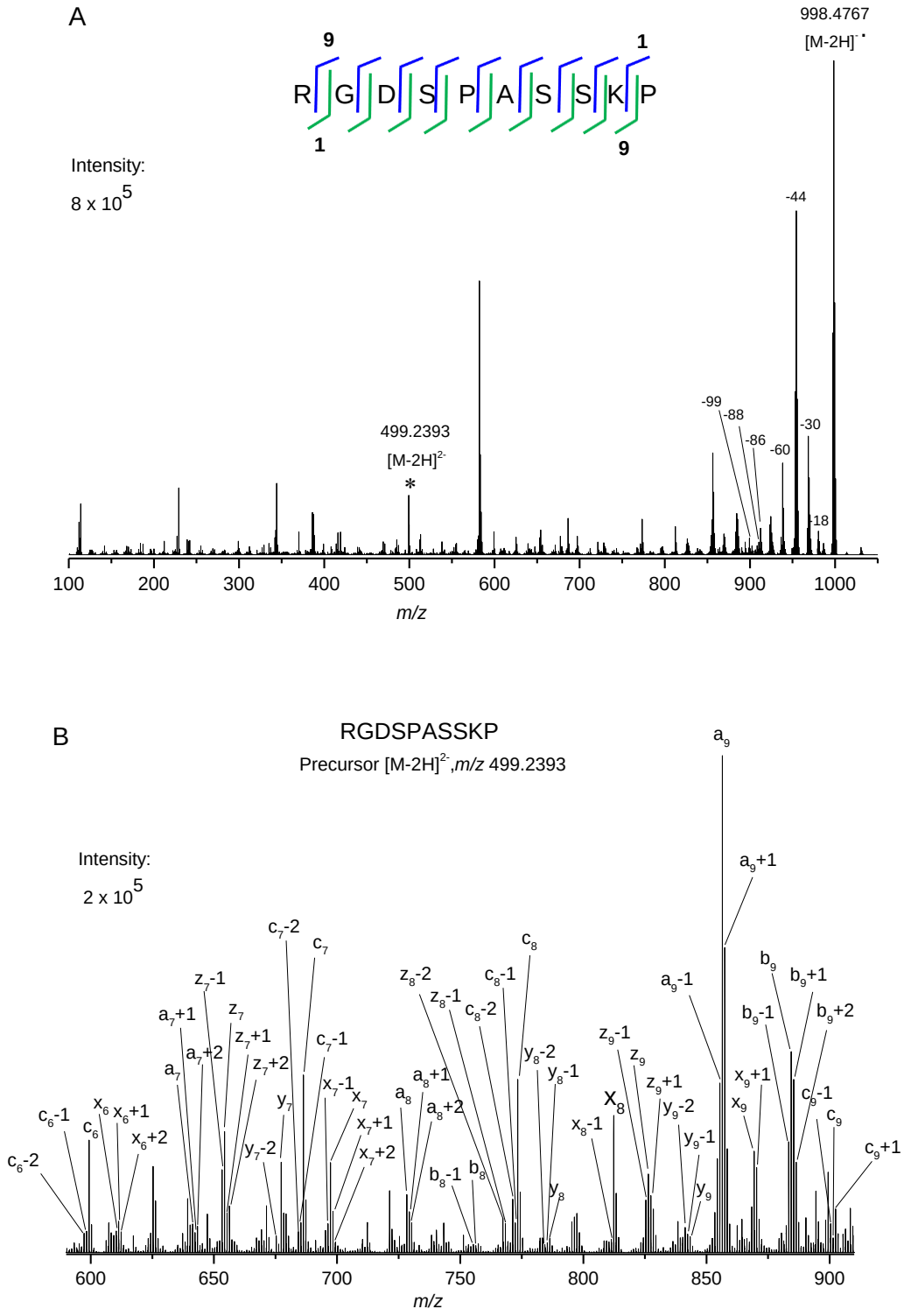

Figure 4. Photodissociation spectra of the doubly-deprotonated $[M-2H]^{2-}$ ion (*m/z*=499.2393) of RGDSPASSKP at 213 nm (the precursor ion is signified by * and neutral losses are indicated by ion masses). The green and blue lines represent the a, b, c and x, y, z ions, respectively.

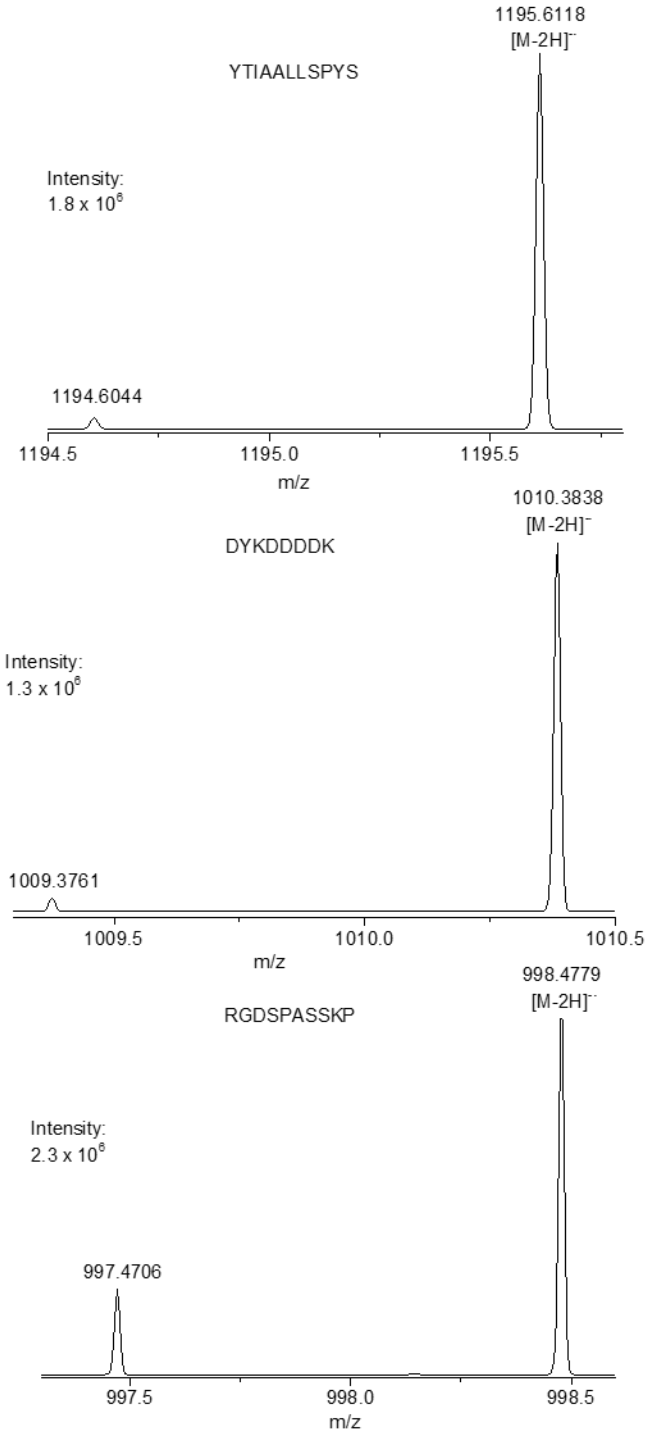

Figure 5: Photodissociation spectra of the doubly-deprotonated $[M-2H]^{2-}$ ion of three peptides. Loss of hydrogen is observed from the characteristic $[M-2H]^{-\bullet}$ charge-reduced radical at single isotope selection of the doubly-deprotonated $[M-2H]^{2-}$ precursor ions.

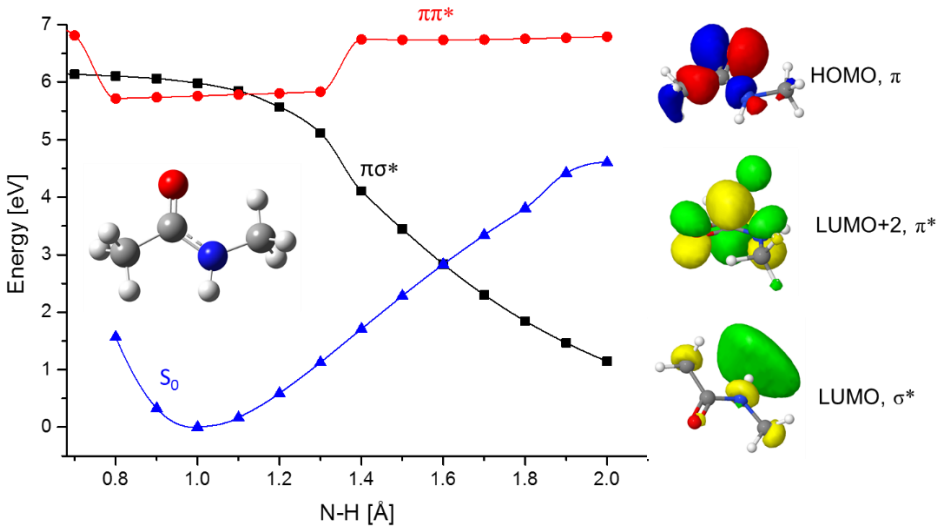

Figure 6: Potential Energy Surface of the lowest ππ*, πσ* and electronic ground state (S_0) as a function of the NH stretch reaction coordinate. The optimization, natural bond orbital (NBO) and TD-DFT calculations have been performed at B3LYP/6-311+G(2d,p) level of theory.

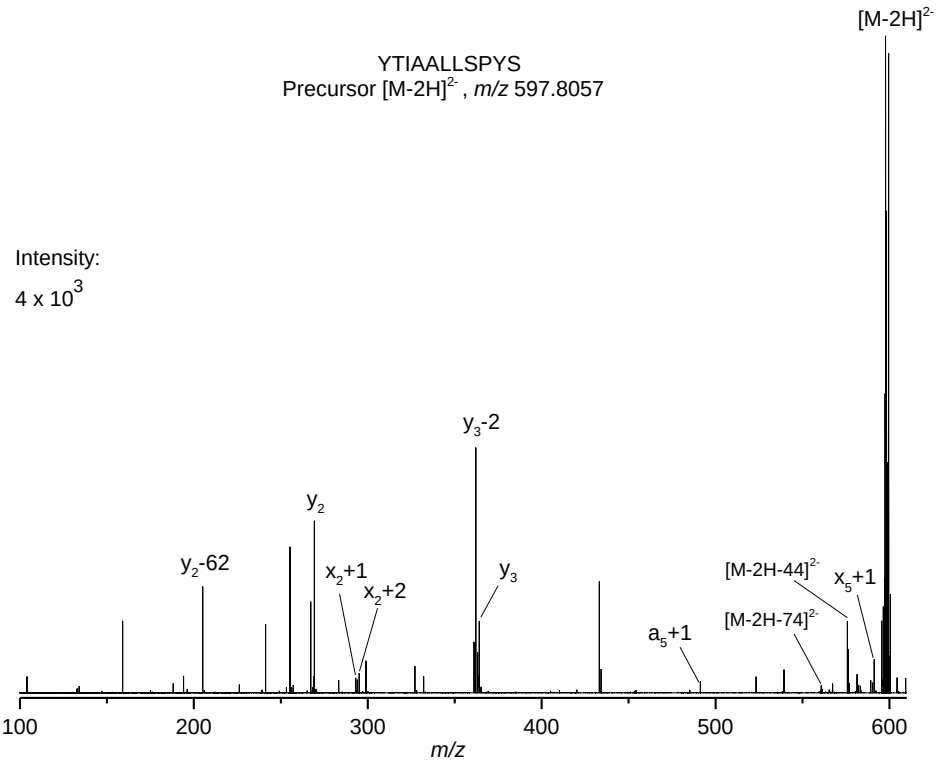

Figure S1. Photodissociation spectrum (*m/z* 100-600) of the doubly-deprotonated $[M-2H]^{2-}$ ion (*m/z*=597.8057) of YTIAALLSPYS at 213 nm.

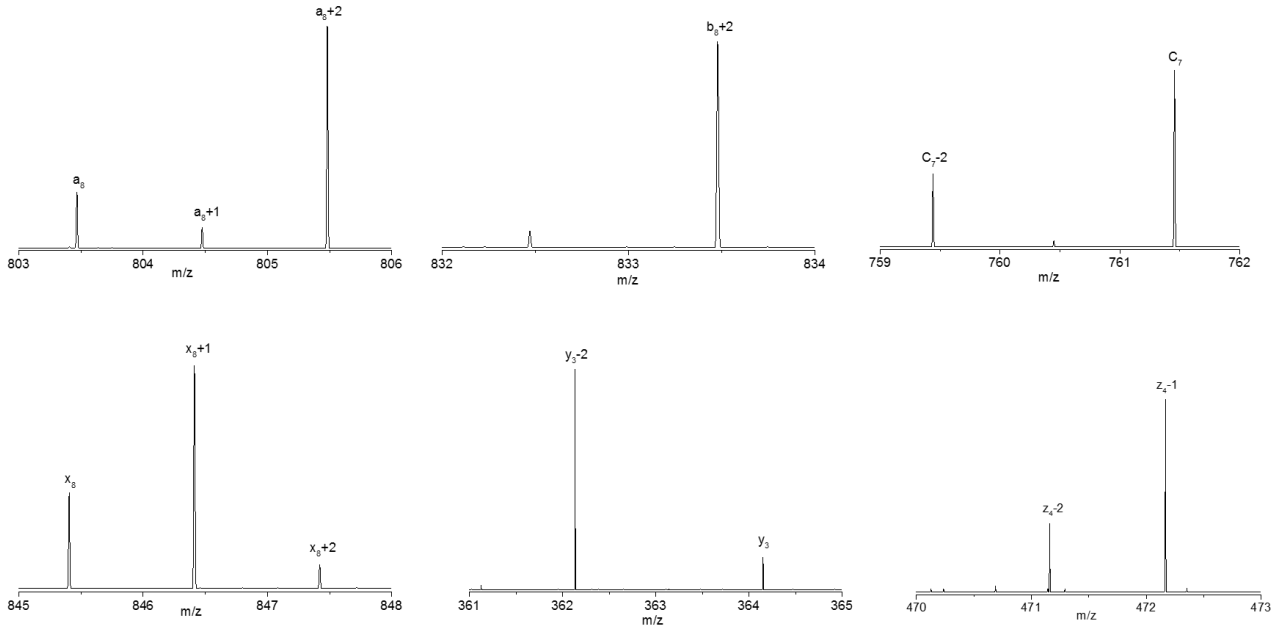

Figure S2: Selected fragment ions from the single isotope selection of the doubly-deprotonated $[M-2H]^{2-}$precursor ions. a/x, b/y and c ions are from peptide 1 and z ion is from peptide 2.

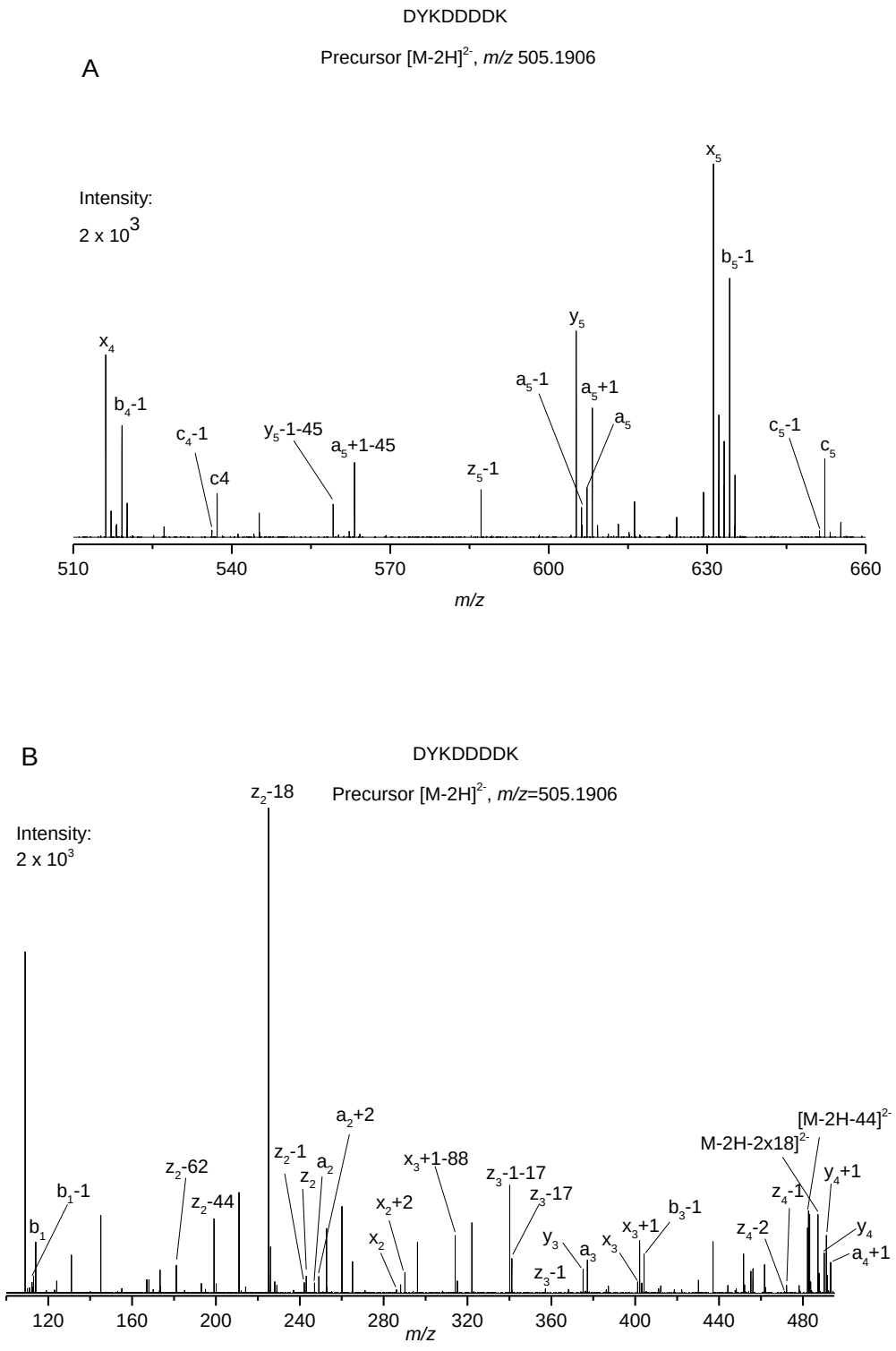

Figure S3. Photodissociation spectra of the doubly-deprotonated $[M-2H]^{2-}$ ion (*m/z*=505.1906) of DYKDDDDK at 213 nm.

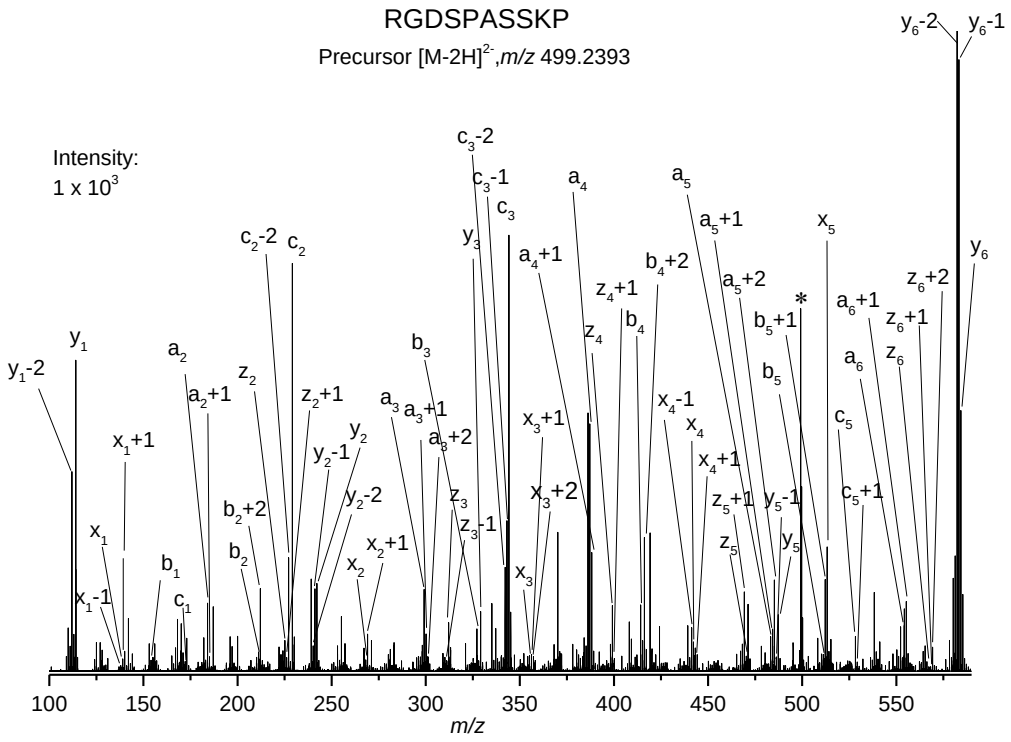

Figure S4. Photodissociation spectra of the doubly-deprotonated $[M-2H]^{2-}$ ion (*m/z*=499.2393) of RGDSPASSKP at 213 nm.

Table S1. Exact masses and assignments of neutral loss detected in the UVPD of doubly-deprotonated (*m/z*=505.1906) of DYKDDDDK $[M-2H]^{2-}$

Experimental m/z	Theoretical m/z	Assignment	Chemical Composition	Mass Difference (ppm)
1010.3812	1010.3829	$[M-2H]^{-\bullet}$	$C_{41}H_{58}N_{10}O_{20}$	-0.6656
992.3709	992.3718	$[M-2H-H_2O]^-$	$C_{41}H_{56}N_{10}O_{19}$	-0.3674
982.3857	982.3874	$[M-2H-CO]^{-\bullet}$	$C_{40}H_{58}N_{10}O_{19}$	-0.6780
966.3913	966.3925	$[M-2H-CO_2]^-$	$C_{40}H_{58}N_{10}O_{18}$	-0.4866
948.3803	948.3819	$[M-2H-(CO_2+H_2O)]^-$	$C_{40}H_{56}N_{10}O_{17}$	-0.6824
939.3099	939.3088	$[M-2H-C_4H_9N]^{-\bullet}$	$C_{37}H_{49}N_9O_{20}$	0.4453
938.3961	938.3612	$[M-2H-C_3H_4O_2]^-$	$C_{38}H_{54}N_{10}O_{18}$	14.0692
922.4019	922.4027	$[M-2H-2CO_2]^-$	$C_{39}H_{58}N_{10}O_{16}$	-0.3296
922.3441	922.3425	$[M-2H-C_3H_6O_2N]^-$	$C_{38}H_{52}N_9O_{18}$	0.6608
910.3076	910.2823	$[M-2H-C_5H_{12}N_2]^-$	$C_{36}H_{46}N_8O_{20}$	10.1959
878.4116	878.4128	$[M-2H-3CO_2]^-$	$C_{38}H_{58}N_{10}O_{14}$	-0.5074
904.3394	904.3405	$[M-2H-(OC_6H_4=CH_2)]^-$	$C_{34}H_{52}N_{10}O_{19}$	-0.4238
903.3321	903.3326	$[M-2H-(HOC_6H_4=CH_2)]^-$	$C_{34}H_{51}N_{10}O_{19}$	-0.2201
886.3281	886.3213	$[x_7-2H_2O]^-$	$C_{38}H_{48}N_9O_{16}$	2.7382
878.3516	878.3526	$[x_7-CO_2]^-$	$C_{37}H_{52}N_9O_{16}$	-0.4247
860.3502	860.3421	$[x_7-(H_2O+CO_2)]^-$	$C_{37}H_{50}N_9O_{15}$	3.2927
820.2853	820.2869	$[a_7+1-H_2O]^{-\bullet}$	$C_{34}H_{44}N_8O_{16}$	-0.6650
819.2776	819.2791	$[a_7-H_2O]^-$	$C_{34}H_{43}N_8O_{16}$	-0.6267
793.2991	793.2999	$[a_7-CO_2]^-$	$C_{33}H_{45}N_8O_{15}$	-0.3062
714.2574	714.2815	$[x_6-COOH]^{-\bullet}$	$C_{28}H_{42}N_8O_{14}$	-9.7102
563.2456	563.2460	$[y_5-COO]^-$	$C_{25}H_{35}N_6O_9$	-0.1707
559.1989	559.1994	$[y_5-1-COOH]^{-\bullet}$	$C_{21}H_{31}N_6O_{12}$	-0.1883

505.1908	505.1912	$[M-2H]^{2-}$	$C_{41}H_{58}N_{10}O_{20}$	-0.1402
496.1855	496.1859	$[M-2H-H_2O]^{2-}$	$C_{41}H_{56}N_{10}O_{19}$	-0.1555
491.1933	491.1937	$[M-2H-CO]^{2-\bullet}$	$C_{39}H_{58}N_{10}O_{17}$	-0.1776
487.1801	487.1814	$[M-2H-2H_2O]^{2-}$	$C_{41}H_{54}N_{10}O_{18}$	-0.5527
483.1955	483.1971	$[M-2H-CO_2]^{2-}$	$C_{40}H_{58}N_{10}O_{18}$	-0.6334
341.1216	341.0979	$[z_3-NH_3]^{-}$	$C_{14}H_{17}N_2O_8$	9.5572
340.1138	340.0901	$[z_3-1-NH_3]^{-\bullet}$	$C_{14}H_{16}N_2O_8$	9.5451
314.1347	314.1585	$[x_3+1-2CO_2]^{-\bullet}$	$C_{13}H_{22}N_4O_5$	-9.5739
225.0868	225.0869	$[z_2-H_2O]^{-}$	$C_{10}H_{13}N_2O_4$	-0.0780
199.1074	199.1077	$[z_2-CO_2]^{-}$	$C_9H_{15}N_2O_3$	-0.1447
181.0967	181.0971	$[z_2-(H_2O+CO_2)]^{-}$	$C_9H_{13}N_2O_2$	-0.1873

Table S2. Exact masses and assignments of ions from backbone dissociation detected in the UVPD of doubly-deprotonated (*m/z*=499.2393) of RGDSPASSKP $[M-2H]^{2-}$.

Experimental m/z	Theoretical m/z	Assignment	Chemical Composition	Mass Difference (ppm)
112.0390	112.0398	$(y_1-2)^-$	$C_5H_6NO_2$	-0.3443
114.0546	114.0555	$(y_1)^-$	$C_5H_8NO_2$	-0.3443
139.0499	139.0269	$(x_1-1)^{-\cdot}$	$C_6H_5NO_3$	9.2655
140.0339	140.0348	$(x_1)^-$	$C_6H_6NO_3$	-0.3421
141.0418	141.0426	$(x_1+1)^{-\cdot}$	$C_6H_7NO_3$	-0.3361
155.0813	155.0933	$(b_1)^-$	$C_6H_{11}N_4O$	-4.8315
172.1192	172.1198	$(c_1)^-$	$C_6H_{14}N_5O$	-0.2683
184.1080	184.1198	$(a_2)^-$	$C_7H_{14}N_5O$	-4.7625
185.1033	185.1277	$(a_2+1)^{-\cdot}$	$C_7H_{15}N_5O$	-9.8397
212.1144	212.1147	$(b_2)^-$	$C_8H_{14}N_5O_2$	-0.1572
214.1188	214.1304	$(b_2+2)^-$	$C_8H_{16}N_5O_2$	-4.6877
225.1237	225.1239	$(z_2)^-$	$C_{11}H_{17}N_2O_3$	-0.0958
226.1315	226.1317	$(z_2+1)^{-\cdot}$	$C_{11}H_{18}N_2O_3$	-0.0897
227.1253	227.1396	$(c_2-2)^-$	$C_8H_{16}N_6O_2$	-5.7478
229.1411	229.1413	$(c_2)^-$	$C_8H_{17}N_6O_2$	-0.0923
240.1347	240.1348	$(y_2-2)^-$	$C_{11}H_{18}N_3O_3$	-0.0591
241.1424	241.1426	$(y_2-1)^{-\cdot}$	$C_{11}H_{19}N_3O_3$	-0.0772
242.1504	242.1505	$(y_2)^-$	$C_{11}H_{20}N_3O_3$	-0.0389
268.1298	268.1297	$(x_2)^-$	$C_{12}H_{18}N_3O_4$	0.0278
269.1251	269.1376	$(x_2+1)^{-\cdot}$	$C_{12}H_{19}N_3O_4$	-5.0372
270.1455	270.1454	$(x_2+2)^-$	$C_{12}H_{20}N_3O_4$	0.0439
299.1468	299.1468	$(a_3)^-$	$C_{11}H_{19}N_6O_4$	0.0129
300.1546	300.1546	$(a_3+1)^{-\cdot}$	$C_{11}H_{20}N_6O_4$	0.0189

301.1625	301.1624	$(a_3+2)^-$	$C_{11}H_{21}N_6O_4$	0.0128
311.1483	311.1481	$(z_3-1)^{-\cdot}$	$C_{14}H_{21}N_3O_5$	0.0602
312.1561	312.1559	$(z_3)^-$	$C_{14}H_{22}N_3O_5$	0.0622
326.1466	326.1339	$(b_3-1)^{-\cdot}$	$C_{12}H_{18}N_6O_5$	5.1204
327.1418	327.1417	$(b_3)^-$	$C_{12}H_{19}N_6O_5$	0.0392
329.1826	329.1825	$(y_3)^-$	$C_{14}H_{25}N_4O_5$	0.0464
342.1527	342.1526	$(c_3-2)^-$	$C_{12}H_{20}N_7O_5$	0.0356
343.1605	343.1604	$(c_3-1)^{-\cdot}$	$C_{12}H_{21}N_7O_5$	0.0416
344.1683	344.1682	$(c_3)^-$	$C_{12}H_{22}N_7O_5$	0.0235
355.1618	355.1618	$(x_3)^-$	$C_{15}H_{23}N_4O_6$	0.0325
356.1694	356.1696	$(x_3+1)^{-\cdot}$	$C_{15}H_{24}N_4O_6$	-0.0825
357.1764	357.1774	$(x_3+2)^-$	$C_{15}H_{25}N_4O_6$	-0.4032
386.1791	386.1788	$(a_4)^-$	$C_{14}H_{24}N_7O_6$	0.1063
387.1868	387.1866	$(a_4+1)^{-\cdot}$	$C_{14}H_{25}N_7O_6$	0.0760
388.1947	388.1945	$(a_4+2)^-$	$C_{14}H_{26}N_7O_6$	0.0982
399.1880	399.1879	$(z_4)^-$	$C_{17}H_{27}N_4O_7$	0.0306
400.1959	400.1958	$(z_4+1)^{-\cdot}$	$C_{17}H_{28}N_4O_7$	0.0366
414.1739	414.1737	$(b_4)^-$	$C_{15}H_{24}N_7O_7$	0.0923
415.1818	415.1815	$(b_4+1)^{-\cdot}$	$C_{15}H_{25}N_7O_7$	0.0984
416.1896	416.1894	$(b_4+2)^-$	$C_{15}H_{26}N_7O_7$	0.1004
441.1861	441.1859	$(x_4-1)^{-\cdot}$	$C_{18}H_{27}N_5O_8$	0.0634
442.1940	442.1938	$(x_4)^-$	$C_{18}H_{28}N_5O_8$	0.0856
443.2018	443.2016	$(x_4+1)^{-\cdot}$	$C_{18}H_{29}N_5O_8$	0.0674
470.2251	470.2251	$(z_5)^-$	$C_{20}H_{32}N_5O_8$	-0.0073
471.2330	471.2329	$(z_5+1)^{-\cdot}$	$C_{20}H_{33}N_5O_8$	0.0391
483.2319	483.2316	$(a_5)^-$	$C_{19}H_{31}N_8O_7$	0.1209
484.2337	484.2394	$(a_5+1)^{-\cdot}$	$C_{19}H_{32}N_8O_7$	-2.2936

485.2429	485.2472	$(a_5+2)^-$	$C_{19}H_{32}N_8O_7$	-1.7511
486.2441	486.2438	$(y_5-1)^{-\cdot}$	$C_{20}H_{35}N_6O_8$	0.1202
487.2521	487.2516	$(y_5)^-$	$C_{20}H_{34}N_6O_8$	0.1746
511.2155	511.2265	$(b_5)^-$	$C_{20}H_{31}N_8O_8$	-4.4115
512.2232	512.2343	$(b_5+1)^{-\cdot}$	$C_{20}H_{32}N_8O_8$	-4.4982
513.2310	513.2309	$(x_5)^-$	$C_{21}H_{33}N_6O_9$	0.0558
528.2534	528.2530	$(c_5)^-$	$C_{20}H_{34}N_9O_8$	0.1476
529.2625	529.2609	$(c_5+1)^{-\cdot}$	$C_{20}H_{35}N_9O_8$	0.6619
553.2618	553.2607	$(a_6-1)^{-\cdot}$	$C_{22}H_{35}N_9O_8$	0.3675
554.2689	554.2687	$(a_6)^-$	$C_{22}H_{36}N_9O_8$	0.0871
555.2766	555.2765	$(a_6+1)^{-\cdot}$	$C_{22}H_{37}N_9O_8$	0.0407
567.2784	567.2778	$(z_6)^-$	$C_{25}H_{39}N_6O_9$	0.2213
568.2723	568.2857	$(z_6+1)^{-\cdot}$	$C_{25}H_{40}N_6O_9$	-5.4128
569.2802	569.2935	$(z_6+2)^-$	$C_{25}H_{41}N_6O_9$	-5.3623
582.2892	582.2887	$(y_6-2)^-$	$C_{25}H_{40}N_7O_9$	0.1973
583.2971	583.2966	$(y_6-1)^{-\cdot}$	$C_{25}H_{41}N_7O_9$	0.1993
584.3047	584.3044	$(y_6)^-$	$C_{25}H_{42}N_7O_9$	0.1247
597.2752	597.2745	$(c_6-2)^-$	$C_{23}H_{37}N_{10}O_9$	0.2712
598.2831	598.2823	$(c_6-1)^{-\cdot}$	$C_{23}H_{38}N_{10}O_9$	0.3014
599.2907	599.2901	$(c_6)^-$	$C_{23}H_{39}N_{10}O_9$	0.2348
610.2845	610.2837	$(x_6)^-$	$C_{26}H_{40}N_7O_{10}$	0.3367
611.2918	611.2915	$(x_6+1)^{-\cdot}$	$C_{26}H_{41}N_7O_{10}$	0.1087
612.2993	612.2993	$(x_6+2)^-$	$C_{26}H_{42}N_7O_{10}$	0.0098
641.3017	641.3007	$(a_7)^-$	$C_{25}H_{41}N_{10}O_{10}$	0.4064
642.3091	642.3085	$(a_7+1)^{-\cdot}$	$C_{25}H_{42}N_{10}O_{10}$	0.2309
643.3171	643.3164	$(a_7+2)^-$	$C_{25}H_{43}N_{10}O_{10}$	0.2813
653.3027	653.3021	$(z_7-1)^{-\cdot}$	$C_{28}H_{43}N_7O_{11}$	0.2682

654.3105	654.3099	$(z_7)^-$	$C_{28}H_{44}N_7O_{11}$	0.2419
655.3183	655.3177	$(z_7+1)^{-\cdot}$	$C_{28}H_{45}N_7O_{11}$	0.2318
656.3124	656.3255	$(z_7+2)^-$	$C_{28}H_{46}N_7O_{11}$	-5.2971
669.3214	669.3208	$(y_7-2)^-$	$C_{28}H_{45}N_8O_{11}$	0.2625
670.3293	670.3286	$(y_7-1)^{-\cdot}$	$C_{28}H_{46}N_8O_{11}$	0.2806
671.3371	671.3364	$(y_7)^-$	$C_{28}H_{47}N_8O_{11}$	0.2827
684.3073	684.3065	$(c_7-2)^-$	$C_{26}H_{42}N_{11}O_{11}$	0.2960
685.3149	685.3143	$(c_7-1)^{-\cdot}$	$C_{26}H_{43}N_{11}O_{11}$	0.2254
686.3226	686.3222	$(c_7)^-$	$C_{26}H_{44}N_{11}O_{11}$	0.1911
695.3001	695.3000	$(x_7-2)^-$	$C_{29}H_{43}N_8O_{12}$	0.0089
696.3084	696.3079	$(x_7-1)^{-\cdot}$	$C_{29}H_{44}N_8O_{12}$	0.2022
697.3161	697.3157	$(x_7)^-$	$C_{29}H_{45}N_8O_{12}$	0.1719
698.3236	698.3235	$(x_7+1)^{-\cdot}$	$C_{29}H_{46}N_8O_{12}$	0.0529
699.3314	699.3313	$(x_7+2)^-$	$C_{29}H_{47}N_8O_{12}$	0.0145
728.3337	728.3327	$(a_8)^-$	$C_{28}H_{46}N_{11}O_{12}$	0.3909
729.3417	729.3406	$(a_8+1)^{-\cdot}$	$C_{28}H_{47}N_{11}O_{12}$	0.4413
730.3494	730.3484	$(a_8+2)^-$	$C_{28}H_{48}N_{11}O_{12}$	0.3909
755.3087	755.3198	$(b_8-1)^{-\cdot}$	$C_{29}H_{45}N_{11}O_{13}$	-4.4984
756.3160	756.3277	$(b_8)^-$	$C_{29}H_{46}N_{11}O_{13}$	-4.6901
767.3457	767.3212	$(z_8-2)^-$	$C_{32}H_{47}N_8O_{14}$	9.8827
768.3531	768.3290	$(z_8-1)^{-\cdot}$	$C_{32}H_{48}N_8O_{14}$	9.7395
769.3361	769.3368	$(z_8)^-$	$C_{32}H_{49}N_8O_{14}$	-0.2837
771.3389	771.3385	$(c_8-2)^-$	$C_{29}H_{47}N_{12}O_{13}$	0.1272
772.3465	772.3464	$(c_8-1)^{-\cdot}$	$C_{29}H_{48}N_{12}O_{13}$	0.0647
773.3546	773.3542	$(c_8)^-$	$C_{29}H_{49}N_{12}O_{13}$	0.1514
784.3483	784.3477	$(y_8-2)^-$	$C_{32}H_{50}N_9O_{14}$	0.2452
785.3564	785.3555	$(y_8-1)^{-\cdot}$	$C_{32}H_{51}N_9O_{14}$	0.3359

786.3650	786.3634	$(y_8)^-$	$C_{32}H_{52}N_9O_{14}$	0.6647
811.3353	811.3348	$(x_8\text{-}1)^{-\cdot}$	$C_{33}H_{49}N_9O_{15}$	0.2049
812.3433	812.3426	$(x_8)^-$	$C_{33}H_{50}N_9O_{15}$	0.2796
825.3753	825.3505	$(z_9\text{-}1)^{-\cdot}$	$C_{34}H_{51}N_9O_{15}$	10.0083
826.3604	826.3583	$(z_9)^-$	$C_{34}H_{52}N_9O_{15}$	0.8524
827.3673	827.3661	$(z_9+1)^{-\cdot}$	$C_{34}H_{53}N_9O_{15}$	0.4672
841.3696	841.3692	$(y_9\text{-}2)^-$	$C_{34}H_{53}N_{10}O_{15}$	0.1791
842.3775	842.3770	$(y_9\text{-}1)^{-\cdot}$	$C_{34}H_{54}N_{10}O_{15}$	0.2053
843.3848	843.3848	$(y_9)^-$	$C_{34}H_{55}N_{10}O_{15}$	-0.0146
855.4221	855.4199	$(a_9\text{-}1)^{-\cdot}$	$C_{34}H_{57}N_{13}O_{13}$	0.8960
856.4281	856.4277	$(a_9)^-$	$C_{34}H_{58}N_{13}O_{13}$	0.1396
857.4357	857.4355	$(a_9+1)^{-\cdot}$	$C_{34}H_{59}N_{13}O_{13}$	0.0689
858.4437	858.4433	$(a_9+2)^-$	$C_{34}H_{60}N_{13}O_{13}$	0.1436
868.3570	868.3563	$(x_9\text{-}1)^{-\cdot}$	$C_{35}H_{52}N_{10}O_{16}$	0.3043
869.3647	869.3641	$(x_9)^-$	$C_{35}H_{53}N_{10}O_{16}$	0.2418
870.3723	870.3719	$(x_9+1)^{-\cdot}$	$C_{35}H_{54}N_{10}O_{16}$	0.1349
883.4153	883.4148	$(b_9\text{-}1)^{-\cdot}$	$C_{35}H_{57}N_{13}O_{14}$	0.2124
884.4231	884.4226	$(b_9)^-$	$C_{35}H_{58}N_{13}O_{14}$	0.1902
885.4307	885.4304	$(b_9+1)^{-\cdot}$	$C_{35}H_{59}N_{13}O_{14}$	0.1236
886.4387	886.4383	$(b_9+2)^-$	$C_{35}H_{60}N_{13}O_{14}$	0.1861
900.4183	900.4413	$(c_9\text{-}1)^{-\cdot}$	$C_{35}H_{60}N_{14}O_{14}$	-9.2759
901.4257	901.4492	$(c_9)^-$	$C_{35}H_{61}N_{14}O_{14}$	-9.4716
902.4337	902.4569	$(c_9+1)^{-\cdot}$	$C_{35}H_{62}N_{14}O_{14}$	-9.3808

Table S3. Exact masses and assignments of neutral loss detected in the UVPD of doubly-deprotonated (*m/z*=499.2393) of RGDSPASSKP $[M-2H]^{2-}$.

Experimental m/z	Theoretical m/z	Assignments	Chemical Composition	Mass Difference(ppm)
998.4767	998.4776	$[M-2H]^{-\bullet}$	$C_{40}H_{66}N_{14}O_{16}$	-0.3643
980.4673	980.4670	$[M-2H-H_2O]^{-}$	$C_{40}H_{64}N_{14}O_{15}$	0.1216
968.4672	968.4670	$[M-2H-CH_2O]^{-\bullet}$	$C_{39}H_{64}N_{14}O_{15}$	0.0611
954.4872	954.4877	$[M-2H-CO_2]^{-}$	$C_{39}H_{66}N_{14}O_{14}$	-0.2218
938.4227	938.4326	$[M-2H-C_2H_6ON]^{-}$	$C_{38}H_{60}N_{13}O_{15}$	-4.0060
912.4072	912.4057	$[M-2H-C_3H_8N_3]^{-}$	$C_{37}H_{57}N_{11}O_{16}$	0.5365
899.3982	899.3979	$[M-2H-C_4H_9N_3]^{-}$	$C_{36}H_{57}N_{11}O_{16}$	0.1210
910.4269	910.4377	$[M-2H-C_3H_6O_2N]^{-}$	$C_{37}H_{60}N_{13}O_{14}$	-4.3368